S-412

# Neutron Physics Section
# Annual Progress Report

October 1, 1968—September 30, 1969

AKTIEBOLAGET ATOMENERGI

STUDSVIK, NYKÖPING, SWEDEN 1970

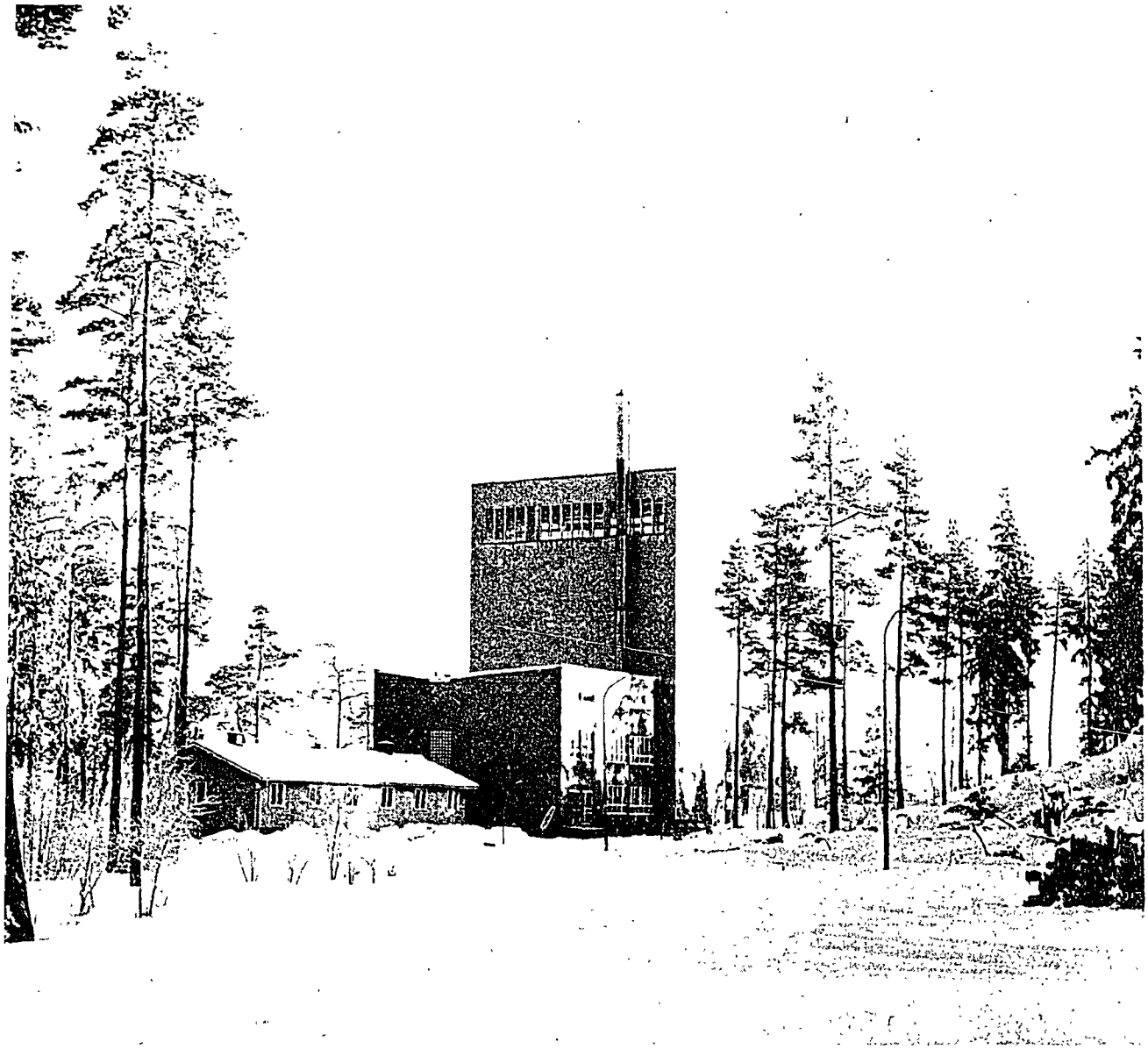

# NEUTRON PHYSICS SECTION

# ANNUAL PROGRESS REPORT

October 1, 1968 - September 30, 1969

Editor: T. Wiedling

Neutron Physics Section
A. B. Atomenergi
Studsvik
Nyköping, Sweden

CONTENTS

# PREFACE

The research program at the Neutron Physics Section is strongly concentrated to problems directly connected with the production of neutron data for the purpose of reactor physics calculations. Thus the elastic and inelastic neutron scattering measurements which have been in progress for many years are still being made to a considerable extent, but also new programs have been initiated, such as the study of neutron capture in the 100 keV region with emphasis on accurate cross section data of reactor elements.

The charge particle (d, pγ) and (d, n) programs have been extended to a study of (d, nγ) reactions by the use of coincidence and neutron time-of-flight techniques.

The (n, p) - and (n, α) - cross sections are of great interest from the reactor physics point of view. However, at present there are only a few measurements of these cross sections for reactor material. One reason is the low neutron flux available from present accelerators. Some promising experiments have been made during the last year by the combination of solid state detectors and time-of-flight techniques. Some theoretical attempts are also made in this field to make up the lack of experimental information.

The $U^{235}$ fission experiment, observing gamma emission from fission fragments, is in many respects unique and is progressing very well. Many interesting properties of the fission process have been observed.

The study of short lived isotopes has continued with extended intensity and effort. With the starting up last summer of the isotope separator on-line the R2-0 reactor the experimental potentialities for this type of experiment have extended appreciably, already giving large amounts of new data.

The channeling effect measurements have continued using protons as well as alpha particles. Studies have been made to localize the positions of impurities in single crystals.

The Van de Graaff accelerator has performed very well as has also the newly installed klystron bunching system.

Physicists from the National Institute of Defense and from several universities in Sweden*, Denmark** as well as many other countries*** have taken the opportunity to use the accelerator facilities.

---

* University of Lund
Chalmers Institute of Technology, Gothenburg
University of Gothenburg
University of Uppsala

** University of Aarhus.

*** Atomic Energy Establishment, Cairo, U.A.R., Egypt
Tehran University Nuclear Centre, Tehran, Iran
Atomic Energy Centre, Ramna, Dacca, East Pakistan

# I. NEUTRON PHYSICS

## I. 1. A SYSTEMATIC STUDY OF FAST NEUTRON ELASTIC SCATTERING IN THE ENERGY REGION 1. 5 TO 8. 1 MeV

B. Holmqvist

Fast neutron elastic scattering angular distributions have been studied in the energy range 1. 5 to 8. 1 MeV from Al, S, Ca, Cr, Mn, Fe, Co, Ni, Cu, Zn, In and Bi, by the time-of-flight technique. The differential elastic cross sections have been determined relative to the well-known neutron cross sections for proton and carbon. The experimental angular distributions have been corrected for the anisotropy of the source neutrons, attenuation of the neutron flux in the scatterer, neutron multiple scattering and for the finite source-sample geometry using a Monte-Carlo computer program.

The experimental material has been used for a systematic study of the nuclear optical model. Theoretical angular distributions have been fitted to the experimental ones, using a local central optical potential consisting of Saxon-Woods, derivative Saxon-Woods, and Thomas form factors describing the real, imaginary, and spin-orbit potentials, respectively. Optimum values of the real and imaginary potential depths, the corresponding nuclear radii, and the real potential diffuseness parameter were calculated independently for each element and energy with an automatic parameter search program. Good agreements have been obtained between the experimental and theoretical angular distributions as shown in Fig. I. 1. 1 for some of the elements. The optical model parameters were found to be essentially independent of the neutron energy except for the even mass number elements for which the real potential depth slowly decreases with the energy. This is demonstrated for some of the elements in Fig. I. 1. 2.

A large amount of information concerning $r_{oU}$, $r_{oW}$ and a has been extracted from the present neutron scattering study. These parameter values have been shown to be mainly independent of the neutron energy apart from minor differences observed at some

However, the discrepancies between the numerical parameter values have not been considered more serious than to allow mean value calculations for each individual element. These mean values of $r_{oU}$, $r_{oW}$ and a are shown in Table I.

Table I. Mean values of $r_{oU}$, $r_{oW}$ and a calculated for each element by taking into account the corresponding optical potential parameter values at all energies studied. The number X signifies the chemical symbol of the element.

| Element | $(\bar{r}_{oU})_X$ | $(\bar{r}_{oW})_X$ | $(\bar{a})_X$ |
|---|---|---|---|
| Al | 1.18 ± 0.01 | 1.22 ± 0.02 | 0.65 ± 0.01 |
| S | 1.20 ± 0.02 | 1.23 } ± 0.04 | 0.66 } ± 0.02 |
| Ca | 1.12 } | 1.34 } | 0.74 } |
| Cr | 1.19 } ± 0.01 | 1.19 ± 0.01 | 0.65 } |
| Mn | 1.19 } | 1.15 ± 0.02 | 0.66 } |
| Fe | 1.20 } | 1.16 ± 0.03 | 0.63 } |
| Ni | 1.19 } ± 0.02 | 1.20 ± 0.02 | 0.69 } |
| Co | 1.24 } | 1.21 ± 0.03 | 0.64 } ± 0.01 |
| Cu | 1.24 } | 1.20 } | 0.68 } |
| Zn | 1.20 } | 1.20 } | 0.68 } |
| In | 1.26 } ± 0.01 | 1.24 } ± 0.01 | 0.65 } |
| Bi | 1.25 } | 1.27 } | 0.66 } |

It is clear from Table I that the values of $(\bar{r}_{oU})_X$, $(\bar{r}_{oW})_X$ and $(\bar{a})_X$ do not fluctuate much from one element to another except for Ca the parameters of which differ significantly. However, since the fluctuations are rather small, it may be assumed that mean values can be calculated for the whole set of parameters. These mean values are $\bar{r}_{oU}$ = 1.21 ± 0.01 fm, $\bar{r}_{oW}$ = 1.21 ± 0.01 fm and $\bar{a}$ = = 0.66 ± 0.01 fm.

The mean values of the optical model geometric parameters have been used in two parameter analyses when varying the real and imaginary potential depths. These investigations were performed at 6.09, 7.05 and 8.05 MeV. The best fits obtained are not essentially different from those obtained in the five parameter analyses. The optimum values of the five parameter (circles) and two parameter

analyses (filled circles) have been plotted versus mass number in Fig. I. 1. 3. It is seen that U decreases somewhat with the mass number and shows a smoother variation in the two parameter than in the five-parameter analyses.

The fluctuation of U may be discussed in terms of the ambiguity relation $Ur_{oU}^2$ at different energies and masses. Outgoing from all elements and energies a mean value of 72 ± 3 MeV $(fm)^2$ was obtained from the five parameter data and the uncertainty is given in such a way that 70 per cent of the products are within the interval $71 \leq Ur_{oU}^2 \leq 75$. More pronounced deviations from the mean value were obtained only for Al, Co and Cu at the two lowest neutron energies and for S below 6 MeV. However, these are the energies and masses where the optical model has a limited validity because of resonance effects. The two parameter data give a mean value of 72 ± 1 MeV $(fm)^2$. The good agreement between the two mean values indicates that $Ur_{oU}^2$ may be considered invariant in the present neutron energy and mass number regions.

The optimum values of U from the two parameter (filled circles) and five parameter (circles) investigations are plotted in Fig. I. 1. 4. as a function of the symmetry parameter $\alpha = (N - Z)/A$ at 6. 09, 7. 05 and 8. 05 MeV neutron energy. It is seen that U is a decreasing function of $\alpha$ at each energy and that the values of U of the five parameter analyses fluctuate somewhat more than those of the two parameter analyses. However, the variations of U with $\alpha$ follow essentially the same trend in the two analyses. The value of $U_1$ in the expression $U = U_o - U_1 (N - Z)/4A$ was estimated from the two parameter data at each energy by least squares fits. The mean value thus obtained is 50 ± 15 MeV, where the error is the largest deviation from the mean value.

In order to avoid the ambiguity of U due to its dependence on $r_{oU}$ the volume integral (J) of the real central potential instead of U has been used as a measure of the strength in a study of the $\alpha$ dependence. The quantity $JU/A = (4\pi U/A) \int_0^\infty f(r) r^2 dr$ was calculated from the data of the five parameter analyses at 6. 09, 7. 05 and 8. 05 MeV neutron energy. These JU/A values are plotted versus $\alpha$ in Fig. I. 1. 5 showing that the strength of the real central potential is a decreasing function of $\alpha$ at each neutron energy. Assuming that JU/A is

linearly dependent on $\alpha$ the slope of the line has been calculated by the least squares method at the three energies studied. The mean value of the slopes of the three lines is 430 ± 40 MeV $(fm)^3$, where the error is the largest deviation from the mean value. From a comparison of Fig. I. 1. 4 with Fig. I. 1. 5 it is evident that the fluctuations of JU/A are smaller than those of U. Thus JU/A seems to be more adequate to use than U when extracting the isobaric spin dependence of the real potential.

The radius is one of the most basic nuclear quantities that can be studied systematically from experimental scattering data. Because of the fundamental interest of the size of the nuclear quantum system it it of interest to compare the neutron interaction radius with those of other probes such as electrons or protons.

Elton [1] has shown that for electron scattering at not too high energies the parameter characterizing the size of the nucleus is not $R_U$ but the root-mean-square (r. m. s.) radius defined by $\langle R_U^2 \rangle = 4\pi \int_0^\infty \rho(r) r^4 dr / 4\pi \int_0^\infty \rho(r) r^2 dr$, where $\rho(r)$ describes the density distribution in the nucleus. Assuming that Elton's expression is valid also for neutron scattering below about 8 MeV the present experimental material has been investigated with respect to the r. m. s. radius by setting $\rho(r) = f(r)$ (the Saxon-Woods form factor) throughout the calculations.

The calculated r. m. s. radii are essentially energy independent allowing a mean value evaluation of $\langle R_U^2 \rangle^{1/2}$ for each element. The variation of $\langle R_U^2 \rangle^{1/2}$ with $A^{1/3}$ is shown in Fig. I. 1. 6 (circles). The straight line represents a least squares fit giving $\langle R_U^2 \rangle^{1/2} = 0.89\ A^{1/3} + 0.96$. For comparison r. m. s. radii calculated with Perey's [2] real optical potential parameters from a study of 17 MeV proton scattering are also included in the figure (filled circles). Perey used the same nuclear potential as here and the parameters were optimized

---

[1] L. R. B. Elton, Nuclear Sizes, Oxford University Press, (1961).

[2] F. G. Perey, Phys. Rev. 131 (1963) 745.

by a $\chi^2$ search procedure. The squares represent the r.m.s. radii given by Greenless et al. [3, 4] from analyses of proton scattering at 11, 30 and 40 MeV. The 11 and 40 MeV radii are only for A = 60. There are good agreements between the results.

---

[3] G.W. Greenless, G.J. Pyle and Y.C. Tang, Phys. Letters 26B (1968) 658.

[4] G.W. Greenless, G.J. Pyle and Y.C. Tang, Phys. Rev. Letters 17 (1966) 33.

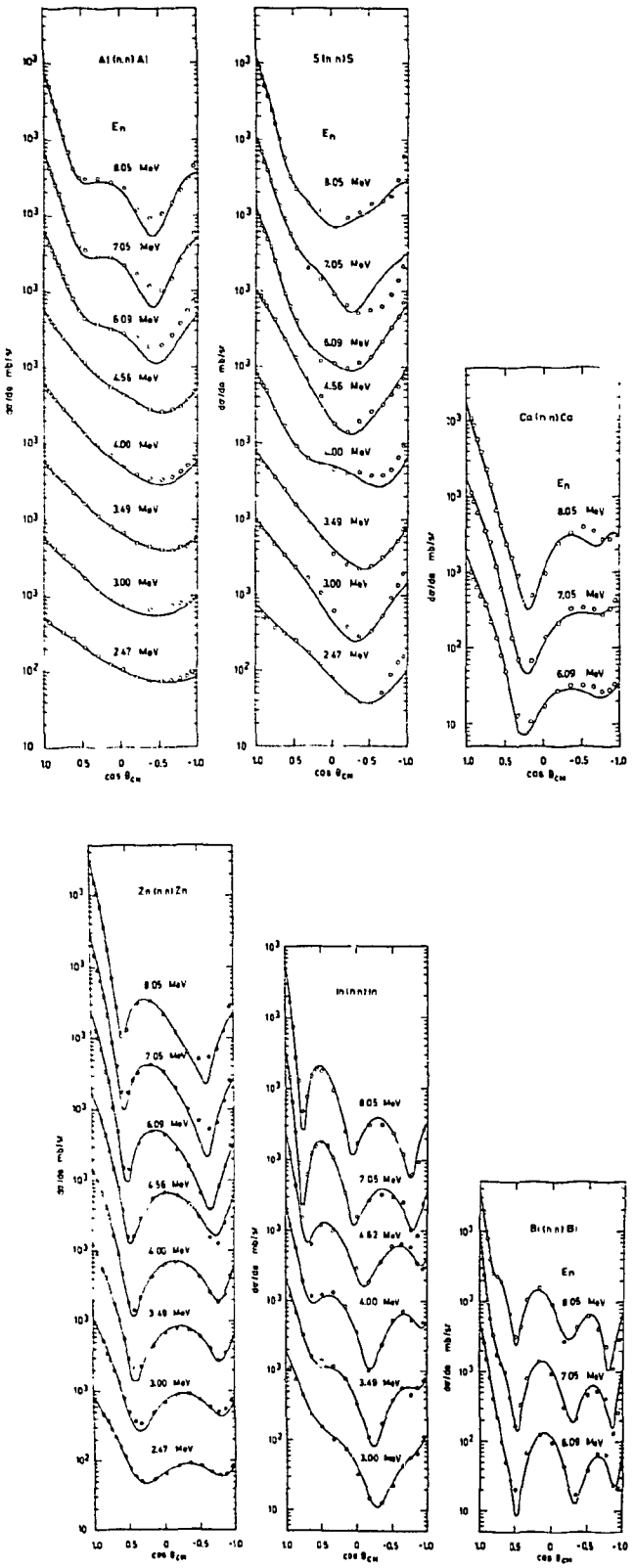


Fig. I.1.1. The experimental and calculated angular distributions of neutrons elastically scattered by Al, S, Ca, Zn, In and Bi. The circles represent the corrected experimental data and the solid lines are the best fits obtained from the optical model calculations.

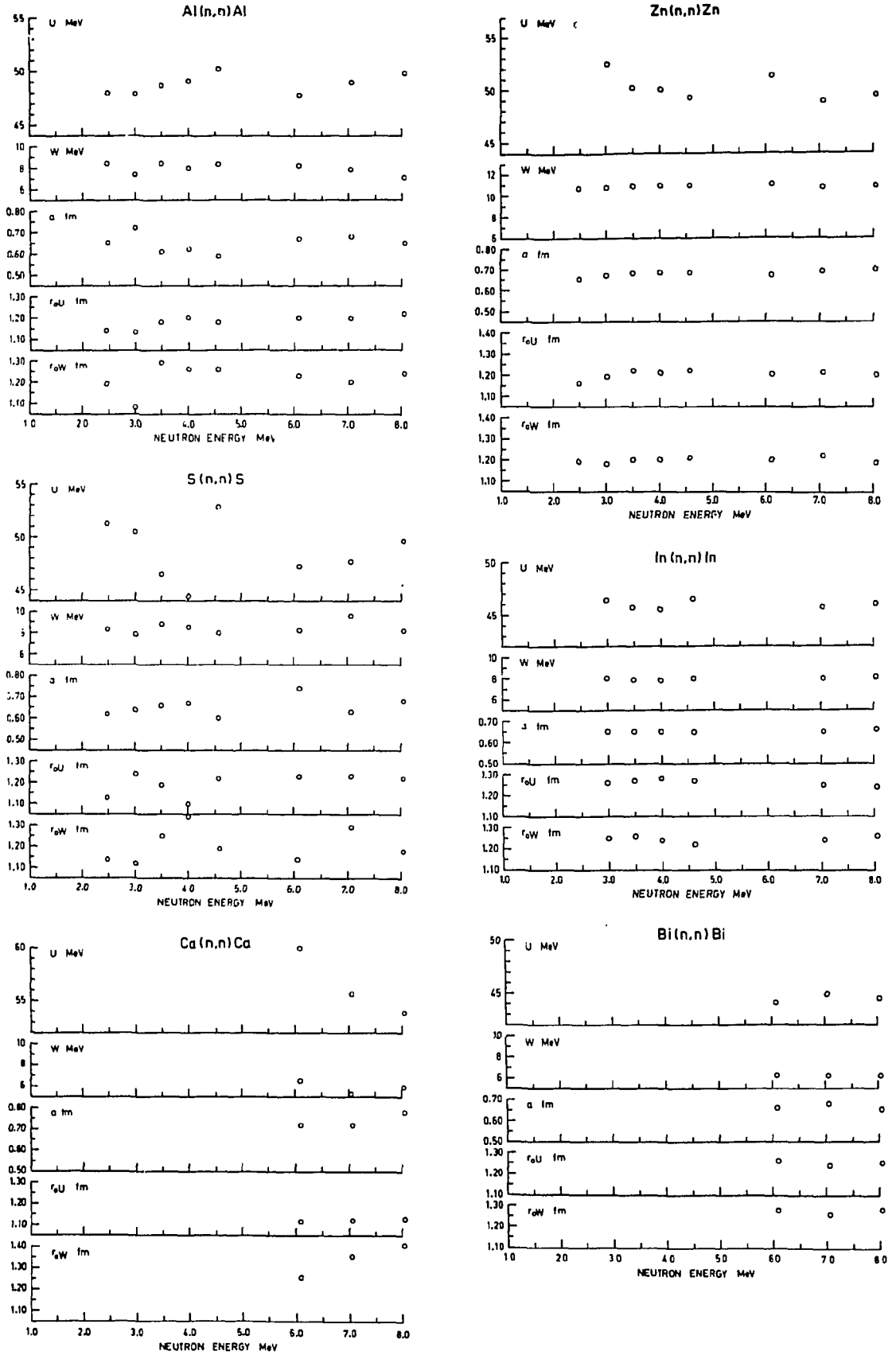


Fig. I.1.2. The optical potential parameter values U, W, a, $r_{oU}$ and $r_{oW}$ of Al, S, Ca, Zn, In and Bi from the five parameter analyses plotted as functions of the neutron energy.

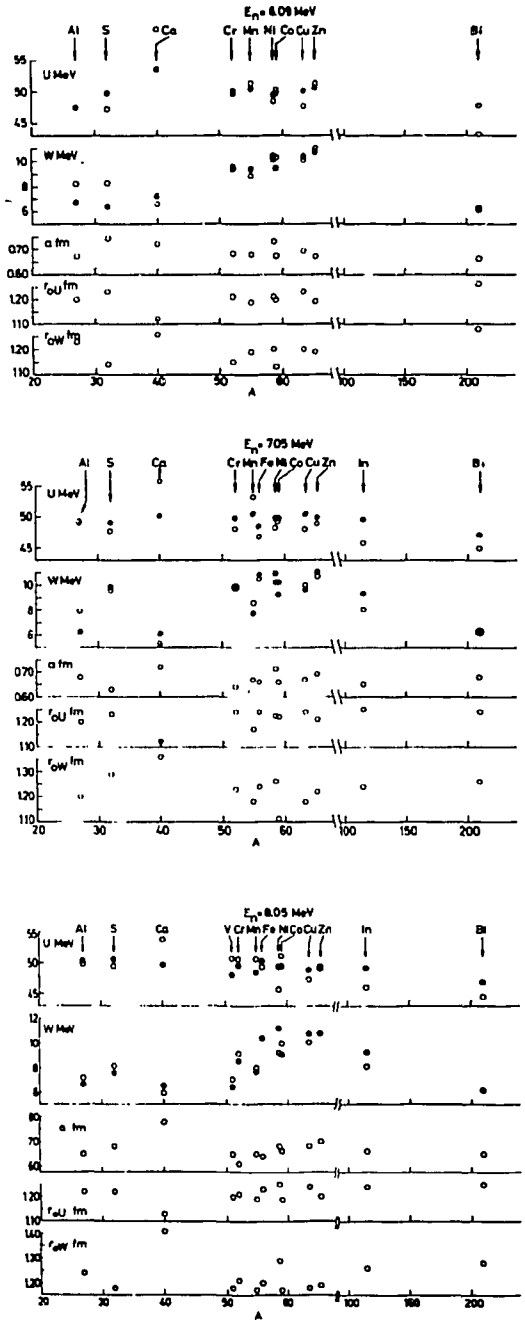


Fig. I. 1. 3. The parameter values of U, W, a, $r_{oU}$ and $r_{oW}$ plotted versus the mass number A (circles) at the neutron energies 6.09, 7.05 and 8.05 MeV. The filled circles are optimum values of U and W obtained from two parameters analyses with $r_{oU} = r_{oW} = 1.21$ fm, a = 0.66 fm and $U_{SO} = 8$ MeV.

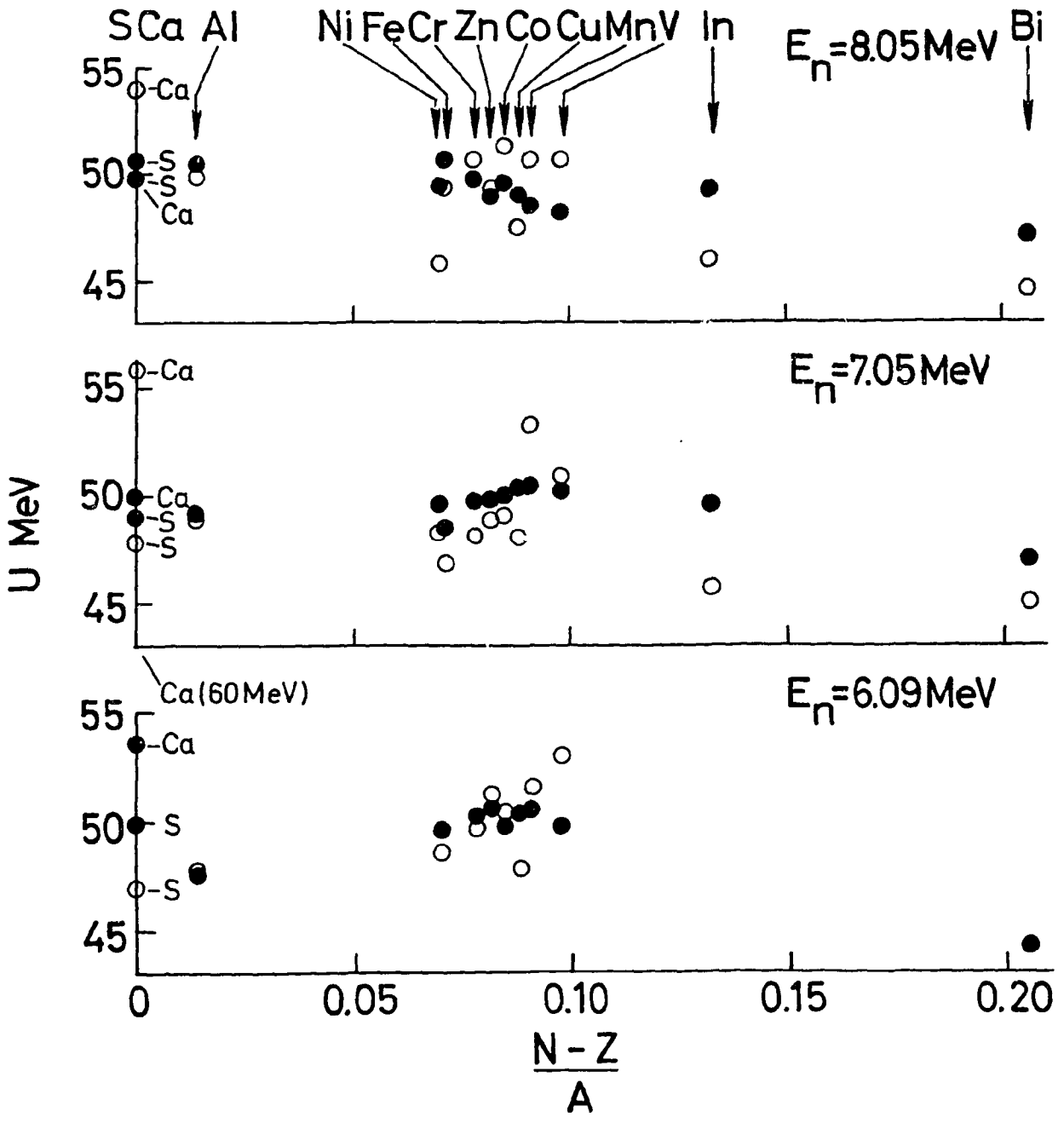


Fig. I.1.4. The optimum values of U from the two parameter (filled circles) and five parameter (circles) calculations plotted as a function of the symmetry parameter (N-Z)/A at 6.09, 7.05 and 8.05 MeV neutron energy.

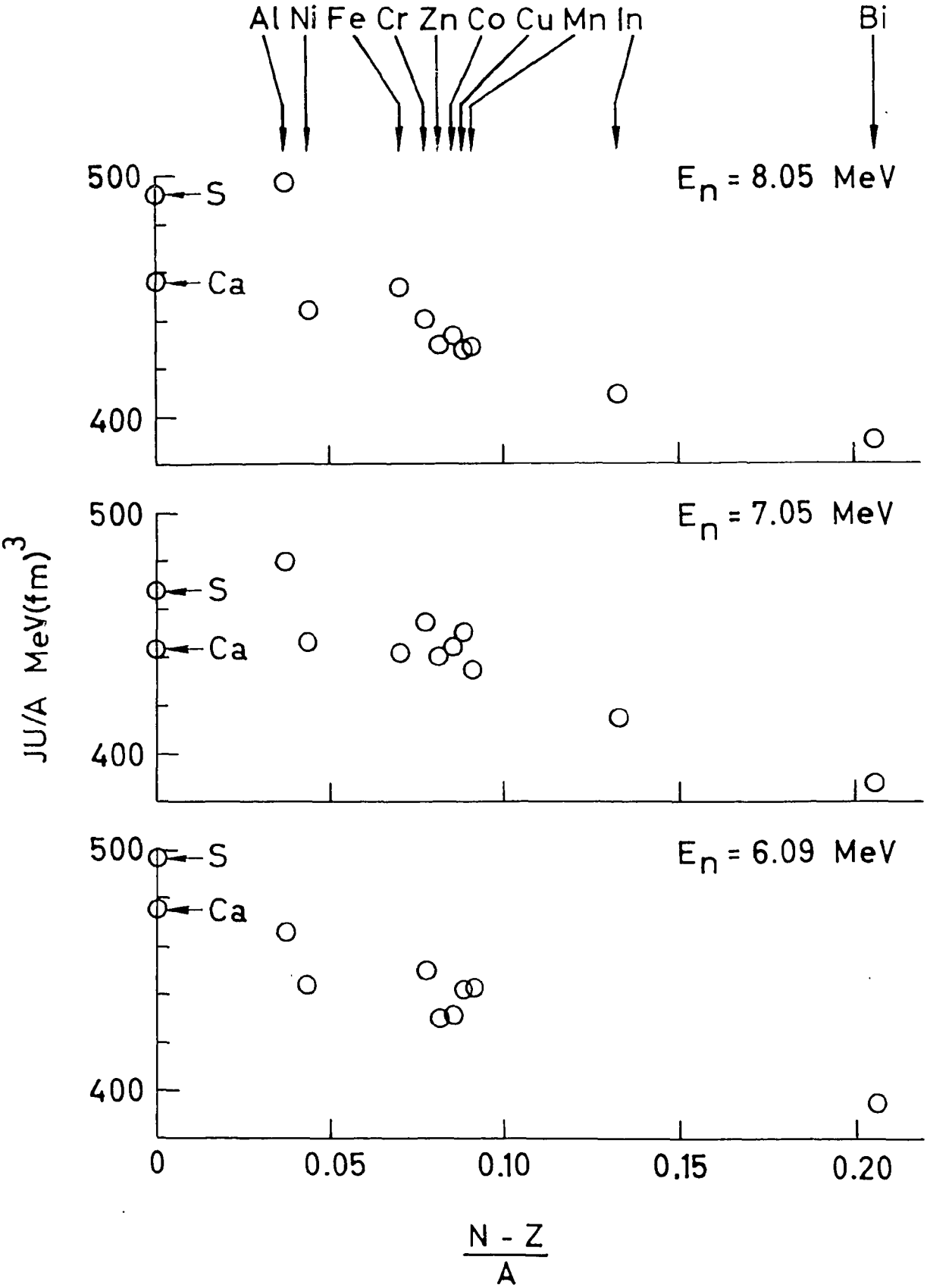


Fig. I.1.5. The quantity JU/A plotted as a function of the symmetry parameter (N-Z)/A at 6.09, 7.05 and 8.05 MeV neutron energy.

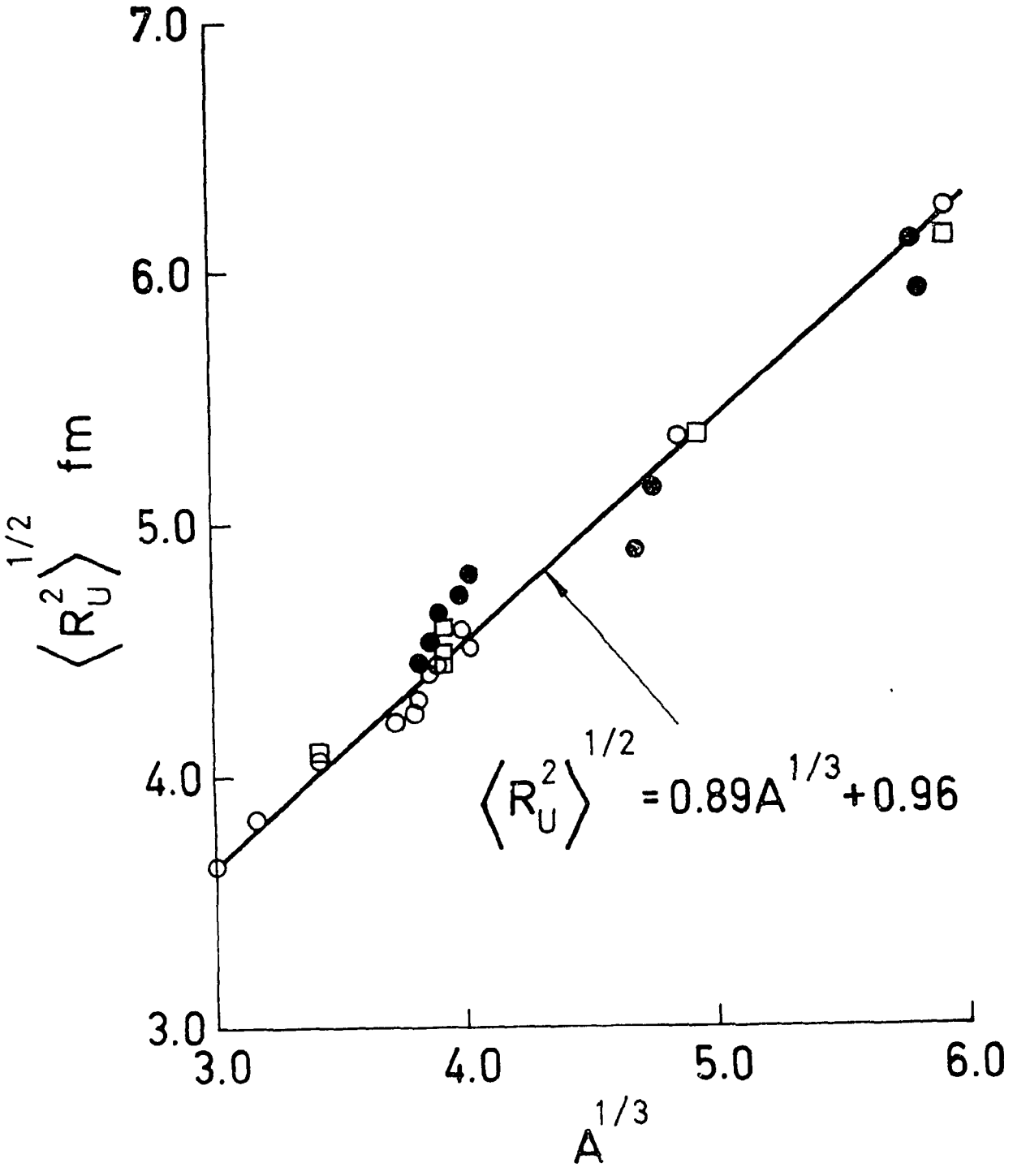


Fig. I.1.6. Mean values of $\langle R_U^2 \rangle^{1/2}$ calculated for each element of the present work plotted versus $A^{1/3}$ (circles). The straight line is a least-squares fit to the points. For comparison the r.m.s. radii calculated with proton optical model data at 17 MeV [2] (filled circles) and at 11.30 and 40 MeV [3, 4] (squares) have been included.

# I. 2 A NON-SPHERICAL OPTICAL MODEL ANALYSIS OF FAST NEUTRON ELASTIC SCATTERING FROM TANTALUM

B. Holmqvist, T. Wiedling
V. Benzi* and L. Zuffi*

A study has been done of the angular distributions of neutrons elastically scattered from the deformed nucleus $Ta^{181}$ at several energies between 2. 5 and 8. 0 MeV.

Because of the large quadrupole moment of strongly deformed nuclei a more realistic model than the spherical optical one must be used to describe the nucleon-nucleus interaction to take the non-spherical nuclear shape into account. Thus the theoretical calculations were performed in the coupled channel adiabatic approximation by assuming a generalized optical potential

$$V(r,\vartheta,\varphi) = -(V+iW)\frac{1}{1+\exp\left[(r-R_a)/a\right]} - 4iW_D\frac{\exp\left[(r-R_b)/b\right]}{\left\{1+\exp\left[(r-R_b)/b\right]\right\}^2}$$

$$-V_{so}(\vec{\sigma}\cdot\vec{\ell})\,\lambda_\pi^2\frac{\exp\left[(r-R_a)/a\right]}{\left\{1+\exp\left[(r-R_a)/a\right]\right\}^2}$$

where the radii $R_a$ and $R_b$ depend on the angle $\vartheta'$ of the body-fixed system as follows

---

*Comitato Nazionale per l'Energia Nucleare, Bologna, Italy.

$$R_a = R_{ao}\left(1 + \beta Y_{20}(\vartheta')\right)$$

$$R_b = R_{bo}\left(1 + \beta Y_{20}(\vartheta')\right)$$

$$Y_{20}(\vartheta') = \sum_{\mu} D^2_{\mu o}(\vartheta_i)\, Y_{2\mu}(\vartheta, \varphi)$$

The quantities $\vartheta$ and $\varphi$ are space-fixed coordinates.

The cross sections are obtained in the usual way by solving the Schrödinger equation with the Hamiltonian

$$H = T + V(r, \vartheta, \varphi)$$

T being the kinetic energy operator.

Due to the angular dependence of the potential on $\vartheta$ and $\varphi$, the Schrödinger equation reduces to a set of coupled differential equations. The adiabatic approximation represented by the omission of the internal motion operator in the Hamiltonian allows the effects of the excited levels belonging to the ground state rotational band to be taken into account in an explicit manner. The effects of the other levels are considered as given by the imaginary part of the optical potential.

The experimental data have been analysed in the light of the optical model with the above mentioned potential as well as with a potential of pure spherical shape.

Cross section calculations with the potential including deformation were performed with the ADAPE code [1] using the following geometrical parameters: $R_{ao} = R_{bo} = 1.25$ fm, $a = 0.65$ fm, $b = 0.48$ fm, $V_{so} = 6$ MeV and $\beta = 0.26$.

Good fits to the experimental data were obtained throughout the energy region with the real and imaginary potential depths of Table I as demonstrated in Fig. I. 2. 1. For comparison the experimental and calculated total and total elastic cross sections have also been included in Table I. The agreements are good between the measured and calculated total cross sections, especially when taking the simplifications adopted in the model into account.

---

[1] F. Fabbri and L. Zuffi, CNEN, Report RT/FI (69) 7 (1969).

Table I. Real and imaginary potential depths of the non-spherical potential used at the different neutron energies. The calculated total cross sections $\sigma_T$ and the total elastic cross sections $\sigma_{el}$ have also been included together with the corresponding experimental quantities.

| $E_n$ MeV | V MeV | $W_D$ MeV | $\sigma_T$ b | $\sigma_{el}$ b | $\sigma_T$(exp) b | $\sigma_{el}$(exp) b |
|---|---|---|---|---|---|---|
| 2.47 | 45.0 | 11.5 | 7.01 | 3.67 | 6.99±0.30 | 3.37±0.24 |
| 3.00 | 45.0 | 11.0 | 6.85 | 3.57 | 6.84±0.20 | 3.07±0.22 |
| 3.49 | 44.9 | 10.0 | 6.68 | 3.45 | 6.70±0.10 | 2.94±0.21 |
| 4.56 | 44.8 | 6.0 | 6.21 | 3.18 | 6.09±0.10 | 3.52±0.25 |
| 6.09 | 44.7 | 6.0 | 5.55 | 2.68 | 5.35±0.10 | 2.39±0.17 |
| 7.04 | 44.6 | 6.0 | 5.35 | 2.52 | 5.18±0.12 | 2.25±0.16 |
| 8.05 | 44.5 | 6.0 | 5.21 | 2.46 | 5.07±0.12 | 2.34±0.17 |

In order to demonstrate the effects of the deformation, calculations were also performed in the framework of the spherical optical model. Thus the parameter values of Table I were chosen as initial values in a five parameter search calculation for constant values of b and $V_{so}$ at 0.48 fm and 6 MeV, respectively. The search procedure was done by using the angular distributions obtained in the calculations with the deformed spherical potentials. The automatic parameter search program ABACUS II was used to optimize the remaining parameters. The results of the calculations are represented by the dashed lines in Fig. I. 2. 1, clearly demonstrating the inadequacy of the spherical model.

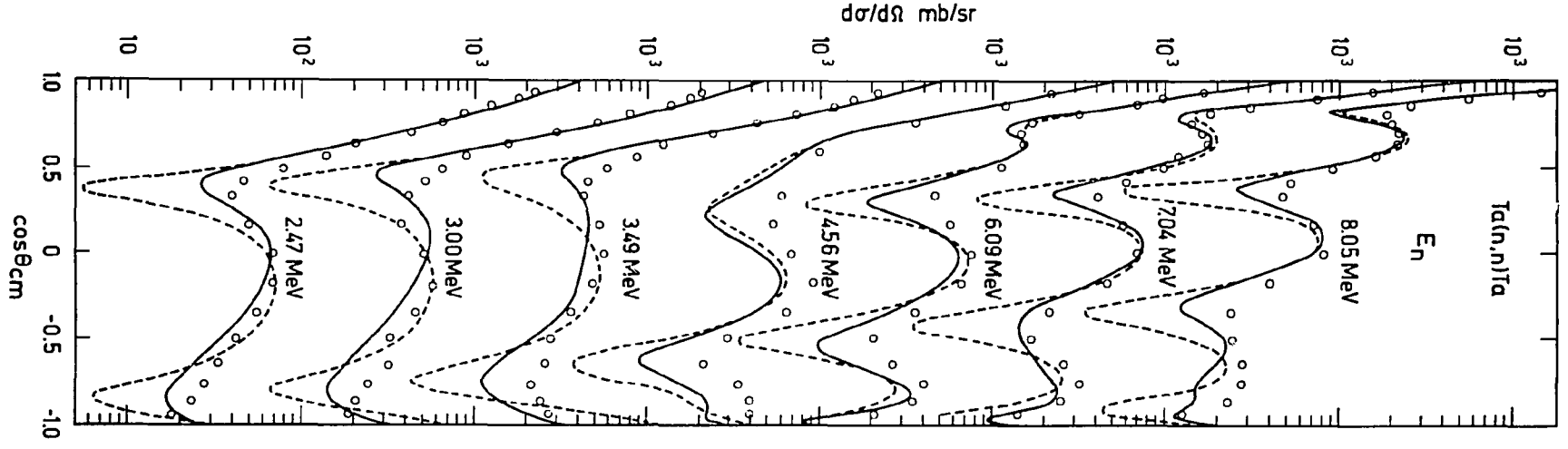


Fig. I. 2. 1 The experimental and calculated angular distributions of neutrons elastically scattered by Ta. The circles represent the corrected experimental data. The dashed lines are the results from calculations with the spherical optical model potential and the solid lines are those with the non-spherical potential.

# I. 3 COMPILATION OF NEUTRON CROSS SECTION DATA MEASURED AT THE STUDSVIK NEUTRON PHYSICS LABORATORY

B. Holmqvist and T. Wiedling

The need for accurate experimental elastic and inelastic neutron cross section data for reactor physics calculations initiated some years ago a program concerning the study of scattering effects of different natural elements in the neutron energy range 1.5 to 8 MeV. Elastic scattering neutron cross section data of the elements Al, S, Ca, V, Cr, Mn, Fe, Co, Ni, Cu, Zn, In, Ta and Bi have been compiled. This work [1] contains information given in tabular form on differential and total experimental elastic scattering cross sections. Included are also Legendre polynominal coefficients. The cross sections calculated by the Abacus II five parameter optical model search routine are tabulated with the optical parameters giving the best fits. The experimental and the calculated elastic scattering angular distributions are also given in graphical form.

---

[1] B. Holmqvist and T. Wiedling, AE-366, EANDC(OR) 92L.

# I. 4 NEUTRON SCATTERING FROM VANADIUM AT 1. 5 TO 8 MeV

B. Holmqvist, S. G. Johansson, G. Lodin and T. Wiedling

The present investigation was undertaken to measure elastic and inelastic neutron scattering angular distributions at several energies between 1. 5 to 8 MeV. However, to obtain the excitation functions of the different levels with good accuracy and within a reasonable time, several points of the excitation curves were measured at one angle only. This was found appropriate because of the small anisotropies of the inelastic angular distribution curves.

The experimental elastic scattering angular distributions have been compared with distributions calculated with a spherical optical model potential consisting of Saxon-Woods and derivative Saxon-Woods form factors describing the real and imaginary potentials, respectively. The spin-orbit interaction was taken into account by a Thomas potential term. The optical potential parameters, i. e. the potential depth, the real and imaginary potential radii and the diffuseness parameter of the real potential, were calculated by using a five-parameter search routine. The spin-orbit potential depth was kept constant, as was also the diffuseness parameter of the imaginary potential. Their values were 8. 0 MeV and 0. 48 fm, respectively. The results of the parameter searches are shown in Fig. I. 4. 1. The agreements between the measured (circles) and calculated (solid lines) angular distributions are good.

Satisfactory agreements were also obtained between the optical model total cross sections and the experimental ones.

The inelastic cross section measurements provide an opportunity to test the Hauser-Feshbach theory when applying the optical model parameters obtained from the measurements of the elastic neutron scattering differential cross sections. The calculated inelastic cross sections have been corrected for the effects of the compound-nucleus level width fluctua-

tions ignored in the Hauser-Feshbach theory. The excitation functions calculated with the modified Hauser-Feshbach theory are compared with the experimental total inelastic cross sections in Fig. I. 4. 2. It is seen that the experimental total inelastic cross sections can be well described in terms of the Hauser-Feshbach theory when the corrections of the level width fluctuations are taken into account and when applying transmission coefficients calculated from an optical potential derived from neutron elastic scattering off the same element.

[1] J.H. Towle, Nucl. Phys. A117 657 (1968).

[2] A.W. Barrows, R.C. Lamb, D. Velkley and M.T. McEllistrem, Nucl. Phys. A107 153 (1968).

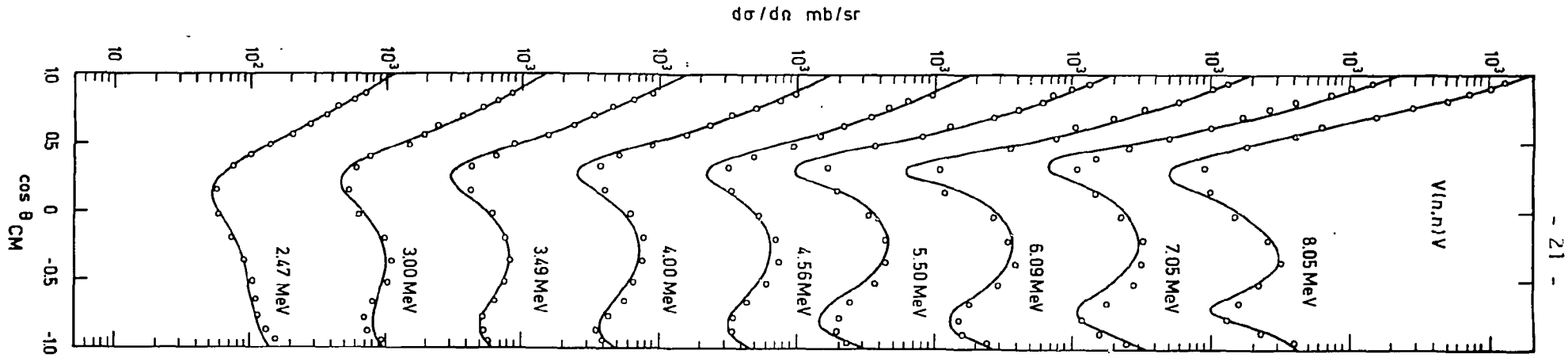


Fig. I. 4. 1 The experimental and calculated angular distributions of neutrons elastically scattered by vanadium. The circles represent the corrected experimental data and the solid lines are the best fits obtained from the optical model calculations.

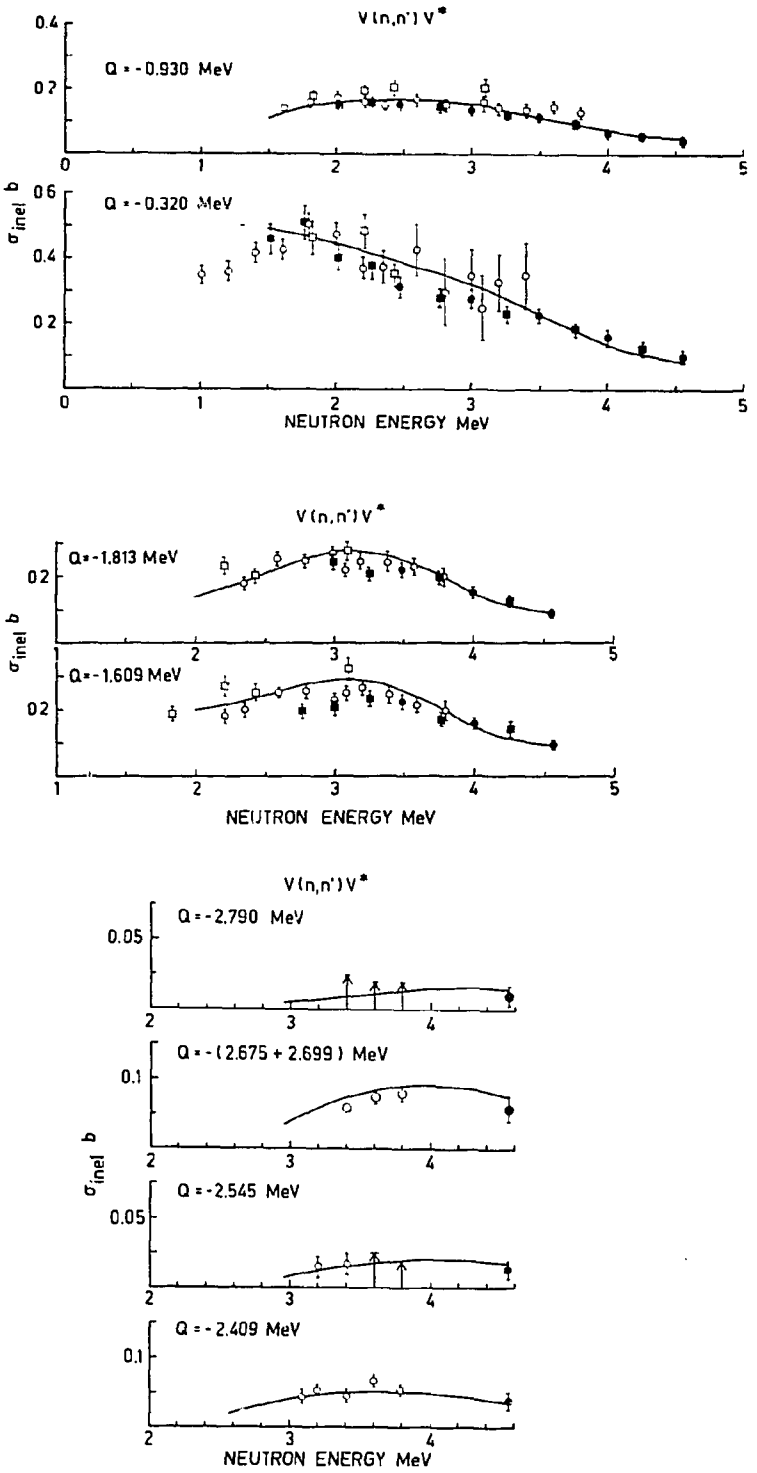


Fig. I. 4. 2. Neutron excitation curves for the 0.320, 0.930, 1.609, 1.813, 2.409, 2.545, 2.675 + 2.699 and 2.790 MeV levels in $V^{51}$. The filled circles and squares are the values from the present work obtained from angular distribution measurements and measurements at one angle only (125°), respectively. The circles and arrows represent the values of Towle [1] and the squares those from Barrows et al. [2]. The solid curves have been calculated with the Moldauer modified Hauser-Feshbach theory.

# I. 5 A NEUTRON ELASTIC SCATTERING STUDY OF CHROMIUM, IRON AND NICKEL IN THE ENERGY REGION 1. 77 TO 2. 76 MeV

B. Holmqvist, S. G. Johansson, G. Lodin,
M. Salama* and T. Wiedling

The elements chromium, iron and nickel are important construction materials in reactor technology. Therefore fast neutron elastic scattering cross sections are required for these elements in the energy region 1–15 MeV and in energy steps of about 50 keV in the low energy region and up to several hundred keV at higher energies.

The purpose of the present investigation was to obtain neutron elastic scattering cross sections of Cr, Fe and Ni at several energies in the 1. 8 to 2. 8 MeV interval where there are only few measurements up to now. Thus elastic scattering angular distributions have been measured for Cr at four energies and for Fe and Ni at five energies in this energy range. This is an extension of work previously carried out at this laboratory on the same elements.

Although the total cross sections of these elements show pronounced resonance structure below about 3 MeV neutron energy it is of interest to compare the measured elastic scattering cross sections with those calculated by means of the nuclear optical model. Thus the observed neutron elastic scattering angular distributions have been compared with distributions calculated when assuming a central local nuclear potential. The experimental distributions have been corrected for the effect of compound elastic scattering by applying the Hauser and Feshbach formalism. The need for width fluctuation corrections has been well documented in a number of experimental efforts in the low neutron energy region, but for Cr, Fe and Ni the experimental angular distributions seem to be better described when using the uncorrected Hauser-Feshbach compound elastic cross sections than those corrected for width fluctuations.

---

* On leave from Reactor and Neutron Physics Department, Atomic Energy Establishment, Cairo, U. A. R., Egypt.

# I. 6 FAST INELASTIC NEUTRON CROSS SECTION MEASUREMENTS ON FISSILE AND NON-FISSILE ISOTOPES

E. Almén, M. Etemad*, B. Holmqvist and T. Wiedling

It has been proposed that the neutron energy spectrum observed in fast neutron fission of $^{235}U$ should be "harder" than earlier expected. For this reason we are at present engaged on measuring fission spectra using time-of-flight techniques. Up to now we have only studied the neutron energy spectrum from $U^{238}$ at 1.35 and 2.0 MeV primary neutron energy. The preliminary analyses show that the fission spectra are well described by Maxwellian distributions. There are no indications of any "harder" spectrum. Further work is in progress.

The fast neutron scattering program is at present concentrated to systematic inelastic scattering measurements. Up to now differential inelastic cross sections have been observed from the elements Al, V, Cr, Mn, Fe, Co, Cu, Zn, Nb, In, Ta and Bi at every 0.25 MeV at neutron energies between 2 and 4.5 MeV. Apart from reactor physics purposes poses the experimental results will be used in a systematic investigation of nuclear models describing the neutron inelastic scattering mechanism.

---

* On leave from Tehran University Nuclear Center, Tehran, Iran.

# I. 7 NEUTRON ELASTIC SCATTERING AT 8 MeV

B. Holmqvist, S. G. Johansson, G. Lodin,
M. Salama* and T. Wiedling

The systematic investigation of the nuclear optical model has been continued by measuring neutron elastic scattering at 8 MeV from the elements As, Nb, Mo, Cd, Sb, Hf, Au, Pb and radiogenic lead.

The analyses of the experimental data were performed with a spherical symmetric potential containing a spin orbit term. The real and imaginary potential depths, the corresponding radii and the real diffuseness parameter were varied to optimize the agreements between the measured and the calculated distributions. These results confirm the isobaric spin dependence of the real potential depth earlier observed [1].

[1] B. Holmqvist, Arkiv Fysik 38, (1968) 403.

* On leave from Reactor and Neutron Physics Department, Atomic Energy Establishment, Cairo, U.A.R., Egypt.

## I. 8. ON THE STUDY OF (n, p) - REACTIONS

G. Lodin* and T. Wiedling

Neutron induced reactions giving charged particle reaction products like protons and alpha particles are of quite large importance in nuclear reactors with their long time integrated intense neutron flux, resulting in serious material destruction. These problems seem to be caused by the gas bubbles from the hydrogen and helium produced. However, at the present time there are rather few measurements of the (n, p) - and (n, $\alpha$) - cross sections of reactor structural materials and at the neutron energies of interest, i. e. from the reaction thresholds up to some MeV. One reason is that the high monoenergetic neutron flux necessary to be able to perform accurate measurements is lacking in most laboratories.

Konijn and Lauber [1] used a surface barrier silicon detector to detect the protons from the Ni (n, p) reaction, but in a rather inconvenient geometry. The technique applied consists of a modification of this technique in the respect that the detector has been placed in a shielded position in relation to the neutron source and that time-of-flight technique has been used in order to be able to ascribe the proton groups to the appropriate neutron energy. The results observed in an experiment with the $^{58}$Ni (n, p) $^{58}$Co reaction at 3. 65 MeV neutron energy are demonstrated in Fig. I. 8. 1. Three spectra are shown, i. e. the proton spectrum (circles) and background obtained with time-of-flight techniques (closed circles), as well as the proton spectrum observed without time-of-flight techniques (small black dots). The proton spectrum shows a pronounced structure, the peaks of which may be identified with proton transitions in the $^{58}$Ni (n, p) $^{58}$Co reaction. The usefulness of the time-of-flight technique is clearly demonstrated. The measuring time for each spectrum is 17 hours.

[1] J. Konijn and A. Lauber
Nucl. Phys. 48, (1963) 191

*Present address: Department of Physics, University of Uppsala, Uppsala

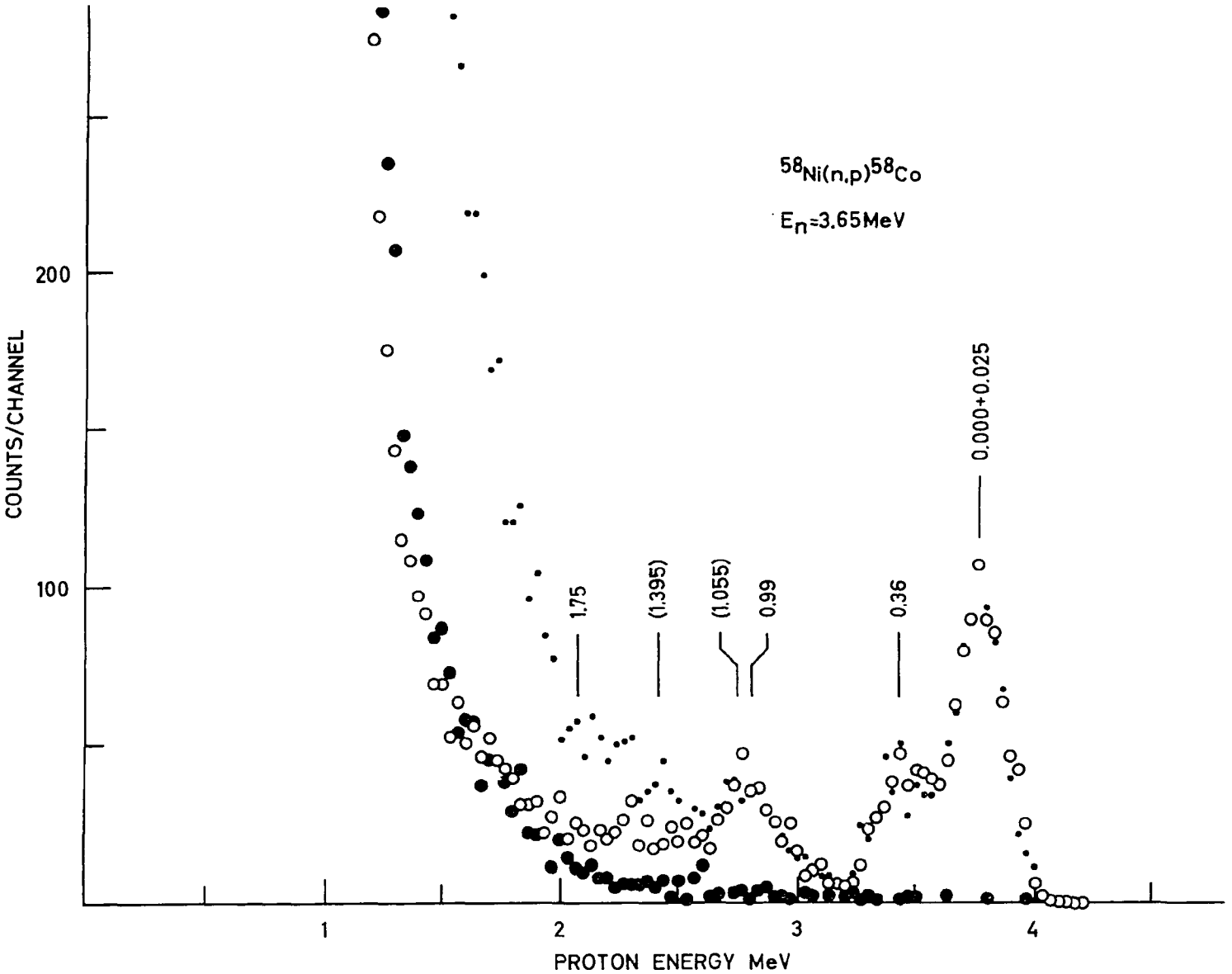


Fig. I. 8. 1. Proton pulse height spectra of the $^{58}Ni(n, p)^{58}Co$ reaction at 3.65 MeV neutron and at 90 degrees laboratory angle. Open and closed circles represent time-of-flight spectra with and without a nickel foil in target position. The small dots represent an ungated proton spectrum.

## I. 9. STUDIES OF NEUTRON CAPTURE

I. Bergqvist*, B. Lundberg**, L. Nilsson and N. Starfelt***

To explain the magnitude of MeV nucleon capture cross sections in medium-weight and heavy nuclei, one is forced to take into account the influence of semi-direct capture processes through the giant dipole resonance. The interaction between the incident nucleon and the target nucleus may excite the latter to its giant dipole resonance while the incident nucleon is captured into a low-lying single-particle orbit. The decay of the giant dipole excitation gives a high-energy gamma-ray transition from the capturing state to a low-lying single-particle state. In a few cases it is possible to study gamma-ray decay to distinct single-particle states. In such cases the comparison with theoretical predictions becomes sufficiently simple to permit definite conclusions concerning the importance of semidirect capture processes.

Gamma-ray spectra from neutron capture in the energy range 1 to 8.5 MeV were recorded for Si, P, S, Ni, $^{206}$Pb and Bi using time-of-flight techniques. The gamma-ray detector is a NaI (Tl) scintillator, 20.8 cm long and 22.6 cm in diameter.

The results for Ni and Bi have been published. The comparison between the experimental cross sections for high-energy gamma-ray transitions from the capturing state to low-lying states in the residual nuclei and calculations based on semi direct capture theories shows that the semi direct capture processes are important for explaining the magnitude and energy variation of the neutron capture cross section in the region of the electric dipole giant resonance.

For the nuclei in the 2s1d shell the analysis is not yet complete. $^{206}$Pb (n,$\gamma$) is a suitable reaction to study the semi direct capture process in the neutron energy range easily achievable by the D(d, n) reaction at the Studsvik Van de Graaff accelerator. The reasons are

---

* Research Institute of National Defence, Stockholm
Present address: Department of Physics University of Lund, Lund

** Research Institute of National Defence Stockholm

*** Present address: Atlas Copco AB, Stockholm

that the neutron binding energy of $^{207}$Pb is 6.7 MeV and that the peak of the giant dipole resonance in $^{206}$Pb is at 13.5 MeV. This means that it is possible to cover an excitation energy region extending up to about 2 MeV beyond the peak of the giant resonance. Preliminary analysis shows that the semi direct capture theory reasonably well accounts for the shapes of the high-energy parts of the gamma-ray spectra. However, the experimental cross sections are about an order of magnitude larger than the cross sections predicted by the semi direct capture theory.

## I.10. THE $^{16}$O(d, n) $^{17}$F REACTION AT DEUTERON ENERGIES FROM 2.5 TO 5.5 MeV

G. Lodin* and L. Nilsson

The $^{16}$O(d, n)$^{17}$F transitions to the ground state and to the first excited state have been studied in the deuteron energy range 2.5 - 5.5 MeV. Time-of-flight techniques and gas target have been used. Differential cross sections in the angular range 0 - 160° at deuteron energies from 3.0 to 5.5 MeV in steps of 0.5 MeV have been recorded as well as yield curves at 0° and 30° from 2.5 to 5.5 MeV in steps of 100 KeV. DWBA calculations using seven different deuteron optical potentials have been performed. It is found that the spectroscopic factors depend strongly on the deuteron optical potential parameter set. Also the ratio between the spectroscopic factors for the transitions to the ground state and to the first excited state is sensitive to this parameter set. The most straight forward choice of deuteron optical potential gives the ratio 1.4 between these spectroscopic factors.

---

* Present address: Department of Physic, University of Uppsala, Uppsala

## I.11. (n, γ)-CROSS SECTION MEASUREMENTS

S. Beshai, S. Malmskog, B. Holmqvist and T. Wiedling

For fast reactor calculations it is of interest to know capture cross sections in the keV region accurately. Such cross sections have up to now mainly been accumulated using pulsed linear electron accelerators as neutron sources. The high energy bremsstrahlung will here via the (γ, n) reaction, create neutrons well up in the MeV region which then have to be moderated to obtain a lower energy neutron spectrum.

An alternative way is to use a charged particle reaction to get a neutron beam of pre-determined energy. It is the intention to use this later method for (n, γ)-cross section measurements with a Van de Graaff accelerator as a neutron source. The produced gamma rays are to be detected in a modified, more effecient Moxon-Rae detector where the detecting medium will be a liquid scintillator stored in a 0.14 $m^3$ cylindrical tank divided into 4 identical counter sections. By imposing different coincidence conditions each counter will have an efficiency proportional to the gamma ray energy, making the detector system independent of the details of the level structure of the final nucleus. The experimental equipment is now being built up and the present status is as follows.

The main scintillation tank has been constructed. Its interior consisting of several concentric cylinders made from 0.5 mm Al sheet has been built and all surfaces have been painted with a reflective coating. Two special end windows have been ordered and will be installed in the middle of January 1970. The liquid scintillator (200 liter of NE 218) will be filled into the cylinder after proper vacuum tests. Eight XP 1040 photomultipliers together with appropriate light guides will be used, while the corresponding eight driving stages have been made. A preliminary block scheme of the full electronic system has been set up and prototypes for a pre-amplifier, a summing circuit and a time-to-pulse-height converter are being built and tested. When the scintillation tank has been finally mounted it will be positioned into a boron-paraffin and lead shielding.

## I.12. (n, γ)-CROSS SECTION MEASUREMENTS USING THE LINEAR ACCELERATOR AT HARWELL

S. Malmskog

During a stay at Harwell during the summer and autumn of 1968 (n, γ)-cross section measurements were performed at the linear electron accelerator at Harwell. A simple type, Moxon-Rae detector, was mounted at a 35 meter flight path station. Using this set up several (n, γ)-cross sections were measured in the energy interval 5 eV-200 keV, in particular $U^{238}$, $Sb^{nat}$, $Ta^{nat}$, $Au^{nat}$ and $Mo^{100}$. Evaluations were made on the IBM 360 computer at Harwell.

A special set up was also made to measure the resonance integral of both Si and SiC.

The later part of the period was devoted to set up a big scintillation tank at a 100 meter flight path station with the aim of studying the (n, γ)-cross section in the MeV region.

# II. NUCLEAR STRUCTURE PHYSICS

## II.1. STUDIES OF (d,pγ) REACTIONS

I. Bergqvist*, L. Carlén**, B. Lundberg***, L. Nauclér** and L. Nilsson

With the aim to achieve an understanding of the neutron capture mechanism in nuclei with mass numbers around 60, (d,pγ) reactions have been studied in $^{58,60}$Ni and $^{63,65}$Cu at 5.5 MeV deuteron energy. The gamma-rays were detected by a NaI(Tl) scintillator, 12.7 cm in diameter and 10.2 cm long, and the protons by a silicon surface-barrier detector of high resistivity. With the use of two-parameter multichannel analysis it was possible to record simultaneously the gamma-ray spectra from several excitation energy regions populated by neutron transfer, in particular those below the neutron binding energies. The gamma-ray spectra from excitation energy regions not too far below the neutron separation energy show strong-intensity high-energy gamma-rays. The shapes of the spectra are similar to those obtained in (n,γ) reactions and disagree with those expected from the theory of the compound-nucleus capture process. Similar experiments have been performed at Chalk River for nuclei with mass numbers around A = 200 and A = 130. Also for these nuclei there is a striking similarity between spectra from (n,γ) and (d,pγ) reactions. It is proposed that a semi direct reaction process proceeding through 2 particle - 1 hole configurations is responsible for a considerable part of the cross section in nuclei around A = 200. In the A = 60 mass region, there is no possibility to determine whether a similar reaction mechanism plays a correspondingly prominent role, since the single-particle strengths are distributed over much larger energy regions than in the A = 200 mass region. A report on the experiment has been published.

* Research Institute of National Defence, Stockholm
Present address: Department of Physics, University of Lund, Lund

** Department of Physics, University of Lund, Lund

*** Research Institute of National Defence, Stockholm

The (d, pγ) studies are being extended to chromium and iron isotopes and to the A = 90 mass region. Preliminary experiments have been performed on natural iron (91.66% $^{56}$Fe) and yttrium (100% $^{89}$Y) and targets of $^{54}$Fe and natural chromium (83.76% $^{52}$Cr) have been ordered. Further experiments are planned for the near future.

## II. 2. NUCLEAR SPECTROSCOPY IN THE 1 f $_{7/2}$ SHELL

B. Erlandsson* and L. Nilsson

The $^{50}$Cr(d,n)$^{51}$Mn and $^{54}$Fe(d, n)$^{55}$Co reactions have been studied at an incident deuteron energy of 5.5 MeV. Angular distributions of neutron groups to a number of low-lying levels in the residual nuclei have been recorded. Time-of-flight techniques have been used to record neutron spectra. A liquid scintillator with pulse-shape discrimination property has been used as neutron detector. DWBA calculations have been performed and relative spectroscopic strengths determined for transitions with various $\ell_p$ values. The ratios between spectroscopic strengths for $\ell_p = 3$ and $\ell_p = 1$ transitions were found to be considerably larger than corresponding ratios obtained from the ($^3$He, d) reactions. Two-step stripping processes competing with the direct stripping process are suggested as explanation of the discrepancy between the (d, n) and the ($^3$He, d) results.

---

* Department of Physics, University of Lund, Lund

## II. 3. STUDIES OF (d, nγ) REACTIONS IN 2s 1d SHELL NUCLEI

I. Bergqvist*, A. Nilsson* and L. Nilsson

Several (p, γ) studies have shown that unbound isobaric analogue states have very simple decay modes. Especially apparent are strong $J \rightarrow J$ M1 transitions from the isobaric analogue states to the so-called anti-analogue states. The (p, γ) reaction does not populate bound isobaric analogue states directly and the secondary population is in general very weak. By means of the (d, n) reaction it is possible to populate these states directly. This reaction also makes it possible to emphasize states with a given orbital angular momentum of the transferred proton by choosing an appropriate angular position for the neutron detector.

A method has been devised to study coincidences between neutrons and gamma rays produced in (d, nγ) reactions. Time-of-flight techniques are used to distinguish neutrons of various energies. The gamma-ray detector is a NaI(Tl) scintillator 20.8 cm long and 22.6 cm in diameter. The method has been used to study $\ell_p = 0$ states in $^{28}$Si and $^{32}$S by means of the $^{27}$Al(d, nγ) $^{28}$Si and $^{31}$P(d, nγ) $^{32}$S reactions. Decay schemes of several $\ell_p = 0, T = 1$ states in $^{28}$Si and $^{32}$S have been determined (Figs. II. 3. 1. - II. 3. 2.).

Similar studies of other 2s 1d shell nuclei are being prepared.

* Department of Physics, University of Lund, Lund.

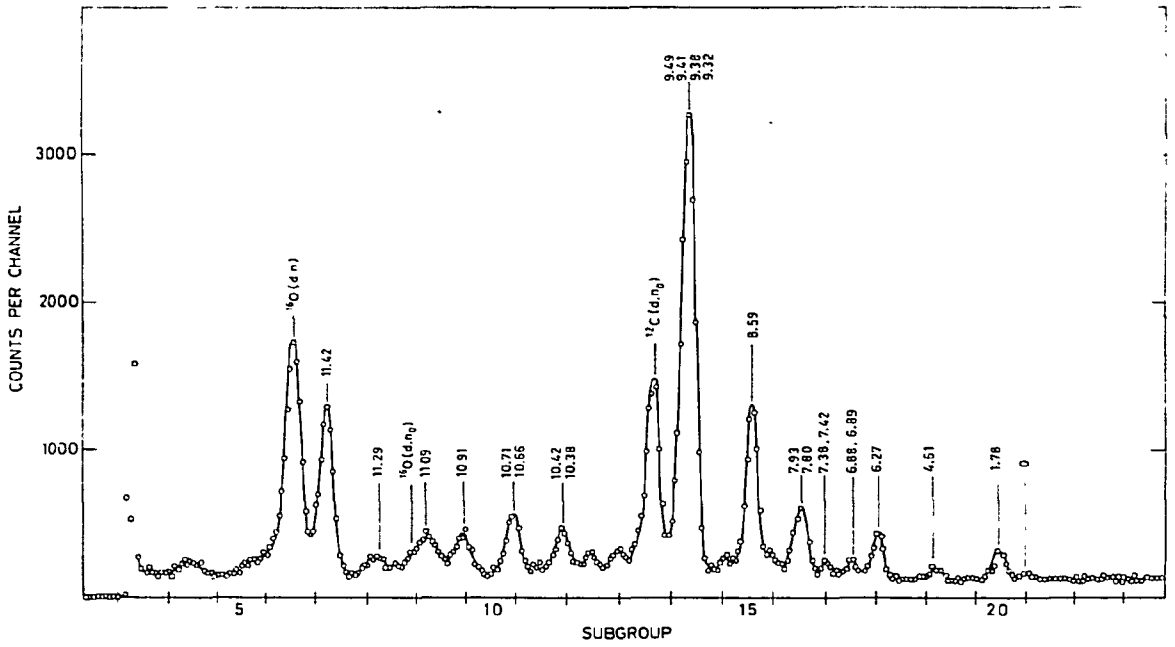


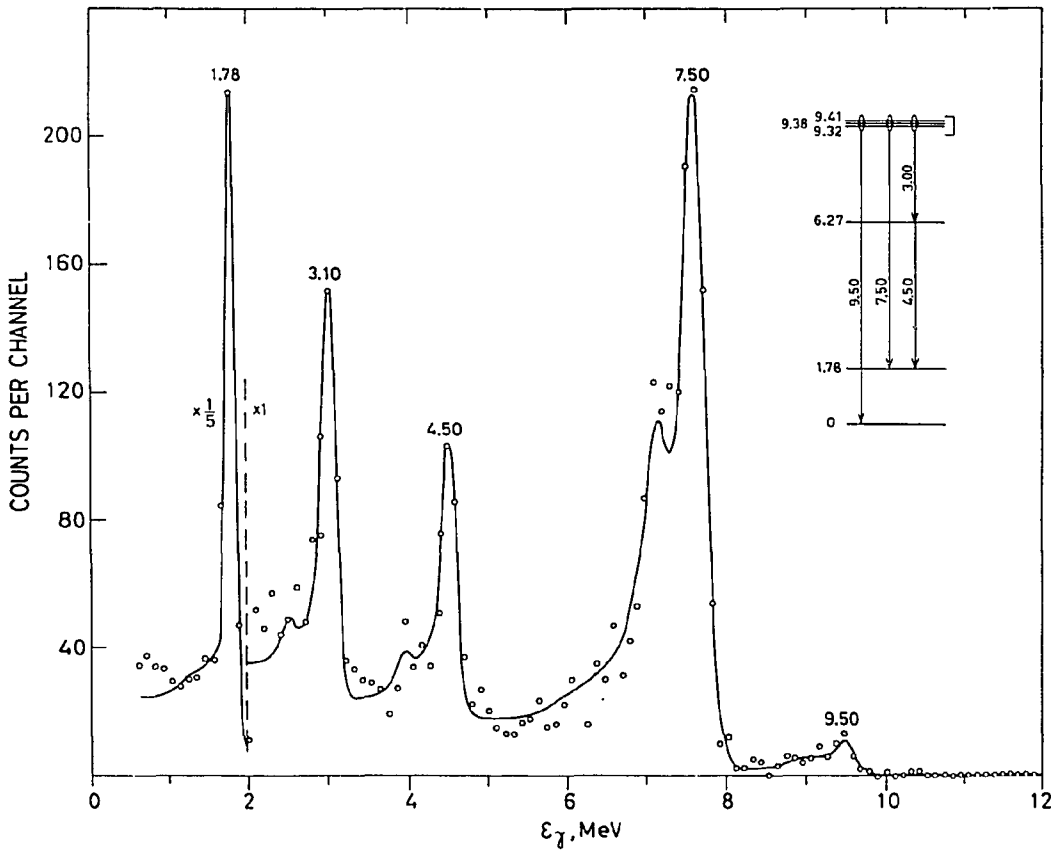


Fig. II. 3. 1. Neutron time-of-flight spectrum from the $^{27}$Al (d, n) $^{28}$Si reaction at the deuteron energy 4.0 MeV and angle 5.0°. Peaks are labelled with the excitation energy of the residual necleus.

Fig. II. 3. 2. The (d, nγ) gammaray spectrum from levels in the excitation energy region $9.0 \leq E_x \leq 9.6$ MeV in $^{28}$Si (essentially from the $\ell_p = 0$, T = 1 levels at 9. 32 and 9. 38 MeV).

# III. NUCLEAR SPECTROSCOPY

## III. 1. BETA AND GAMMA-RAY SPECTROSCOPY

S. G. Malmskog, V. Berg*, Å. Höglund* and J. McDonald**

The experimental studies of decay properties of radioactive nuclei using beta spectrometers, Ge(Li) detectors and delayed coincidence techniques for half-life measurements are being continued.

During this period the main effort has been to study activities produced in the on-line mass separator facility OSIRIS attached to the reactor R2-0 at Studsvik. Both off-line and on-line measurements have been performed, the latter method being used for activities with half-lives below 1 min.

Parallel to these studies measurements on mass separated sources from the ISOLDE project at CERN have progressed. Activities with half-lives longer than 10 hours produced from the spallation of lead have been systematically investigated.

Short reviews of performed experiments are given below.

### $La^{141}$

The half-life of the 190 keV level has been found to be 1.27 ± 0.05 ns. Conversion electron measurements have shown that the 190 keV transition is of M1 multipolarity with less than 8 % E2 admixture. The gamma-ray spectrum below 800 keV following the decay of $^{141}Ba$ has been studied using a 1.5 $cm^3$ Ge(Li) detector and gamma-rays of the following energies have been found: 163.1, 180.4, 190.1, 276.6, 303.8, 343.3, 457.2, 461.8, 466.8, 624.5, 647.2 and 738.4 keV. These have been placed in a decay scheme with levels at 190.1, 303.8, 466.8, 647.2 and 928.5 keV.

### $^{134}I$

Half-life measurements in $^{134}I$ have given the following results:

---

* Department of Physics, University of Stockholm

** Post fellowship from the Royal Society of Physics, London, England

$T_{1/2}$ (79.5 keV level) = 1.62 ± 0.05 ns

$T_{1/2}$ (181.1 keV level) < 100 ps

$T_{1/2}$ (210.8 keV level) < 150 ps

$^{91}$Sr

Properties of the first excited state in $^{91}$Sr have been studied in the decay of $^{91}$Rb ($T_{1/2}$ = 58.2 sec) produced in fission and mass separated in the OSIRIS on-line facility. This level was found to have an energy of 93.54 keV with $T_{1/2}$ = 88 ± 3 ns. It is thought to be a $(2d_{5/2})^3$ particle configuration state.

$^{151}$Eu

High-resolution spectroscopy has been performed in the decay of $^{151}$Gd. Four new transitions have been observed requiring two new levels in $^{151}$Eu. The following half-lives were obtained $T_{1/2}$ (21.6 keV) = 9.4 ± 0.4 ns, $T_{1/2}$ (243.6 keV) = 0.36 ± 0.02 ns and $T_{1/2}$ (350.3 keV) ≤ 0.1 ns.

$^{182}$Ta

Lifetimes of several high energy levels in $^{182}$W have been measured. The data is still being processed.

$^{193}$Hg and $^{195}$Hg (in collaboration with Bäcklin *)

L and M subshell ratios and half-lives have been measured for the 39.49 keV transition in $^{193}$Hg and the 37.13 keV and 16.21 keV transitions in $^{195}$Hg. A systematic compilation of reduced E2 and M1 transition probabilities in odd mass Pt, Hg and Pb nuclei is given and the data are compared to theoretical predictions.

Ir$^{188}$

Half-lives of several excited levels in $^{188}$Ir have been measured using an electron-electron delayed coincidence spectrometer. Active $^{188}$Pt sources were prepared from spallation products using the ISOLDE

---

* The Swedish Research Council Laboratory

on-line mass separator facility at CERN. The following half-lives were observed.

$T_{1/2}$ (54.8 keV) = 1.93 ± 0.10 ns

$T_{1/2}$ (96.7 keV) = 1.59 ± 0.12 ns

$T_{1/2}$ (187.6 keV) = 0.056 ± 0.013 ns

$T_{1/2}$ (195.1 keV) = 0.051 ± 0.010 ns

$T_{1/2}$ (178.3 keV) ≤ 0.15 ns

$^{189}$Ir, $^{189}$Os, $^{187}$Os and $^{185}$Os (in collaboration with Bäcklin*)

All sources were produced at ISOLDE. Extensive investigations with both β- and γ-spectroscopy have been performed. All decays were found to be very complex, with more than 100 transitions in the decay of each isotope. Half-lives of several excited levels have also been measured. The evaluation of the data is still going on.

$^{192}$Hg (in collaboration with Bäcklin*)

Recently the half-life and the multipolarity of the 31.5 keV transition has been measured. Data is being processed.

$^{121}$Sn, $^{128}$Sb, $^{130}$Sb and $^{130}$Te

These nuclei are being studied in the decay of fission products. In each of these nuclei a new isomeric level has been observed, the position of which is being further studied.

A general survey of the activity produced in the low mass peak from $^{235}$U (n, fission) is being carried out at OSIRIS. Several new isotopes have been observed, generally with half-lives shorter than 10 seconds.

---

* The Swedish Research Council Laboratory

## III. 2. PROMPT GAMMA RADIATION FROM FISSION FRAGMENTS

H. Albinsson* and L. Lindow

During recent years more and more attention has been drawn to the study of the gamma radiation from fission fragments. These studies have particular interest for two reasons. The first is that these nuclei cannot be produced in other reactions and radiation from them yields information about states in nuclei far off the line of beta stability. The second reason is that the fragments will give increased knowledge of the systematics of nuclear structure.

With the advent of the solid state detectors of the surface barrier type it is now possible to measure with improved accuracy different kinds of radiation, such as alpha and gamma, in coincidence with the fission fragments. In the experiment described in the present report the prompt gamma radiation from the fragments has been investigated. The term "prompt radiation" used here means that we are dealing with half-lives shorter than about $10^{-9}$ s. This limit is arbitrary, but in californium fission [1 ] it was found that the gamma radiation could be divided into two parts: a prompt component with a half-life shorter than $10^{-9}$ s, and a delayed component. As the average velocity of the fragments is $10^{9}$ cm/s this means that we are studying gamma radiation from the fragments within a flight path of about 1 cm from the fission foil.

The prompt gamma radiation, emitted from fission fragments in slow neutron induced fission of $^{235}U$, was studied as a function of fragment mass and time after fission. The uranium, enriched to about 95 % $^{235}U$, was electrodeposited on 100 $\mu g/cm^2$ nickel foils. The fissile deposit was in all runs less than 100 $\mu g/cm^2$ and one $cm^2$ in area. Two solid state detectors of the surface barrier type were placed in parallel and symmetrically around the fission foil to detect the energies of the fragments. A gamma detector, a NaI scintillator, was placed perpendicular to the plane containing the direction of the neutron beam and the direction of the motion of the detected fragments. The gamma quantas were detected in coincidence with fission events. The NaI scintillator

---

* Chalmers University of Technology, Göteborg

[1 ] Johansson, S.A.E., Nucl. Phys. 60 (1964) 378.

was placed about 70 cm from the fission foil in order to get time discrimination between the fission gammas and the prompt neutrons released in the fission process. The time separation at the NaI scintillator between the prompt photons and the prompt neutrons was about 35 ns. The gamma radiation emitted in different time intervals after the fission events was studied by changing the position of a collimator along the path of the fission fragments. In this way it was possible to get estimates of the life times of the gamma-emitting states. The fission foil, the fragment detectors, and the collimator were all enclosed in an evacuated fission chamber.

The time distribution of the gamma radiation has been studied by the above-mentioned recoil distance method. Time-of-flight spectra were accumulated with different collimator settings and the intensity variation of the gamma peaks was a measure of the intensity as a function of the time intervals after fission which were studied. Three main decay components have been found so far, having tentative half-lives of 7, 20 and 50 ps. Measuring the fastest radiation was more a mechanical than any other problem. The collimator had to be narrow - we used 0.15 mm - and well aligned with the plane of the foil. The foil had to be plane and its surface must have no shrinkles. The adjustment was made in a darkroom with light falling through the collimator slit, and by moving the foil "to" the collimator it was possible to see when and how the light "touched" the foil. Every little speck of dust and wrinkle on the foil first came into the light and reflected it from points and small areas. If the foil was smooth, clean and well aligned, the reflection of the light came gradually from the whole surface.

This tedious and circumstantial procedure was done only once for every series of measurements, namely at its start. The decay curve was then obtained from the time-of-flight spectra, which in turn were recorded for consecutive collimator settings controlled by a micrometer screw. The accuracy of the screw is one part in 0.01 mm. The settings of the collimator were made in one direction, so that it was possible to benefit from the precision of the micrometer screw, and relative to one another the accuracy of the settings was of that order. The analysis of the data is not yet complete. It will include corrections for the collimator geometry and the fragment velocity distribution.

In some of the measurements the time-of-flight spectra were accumulated as a function of gamma-ray energy. The energy region was mostly from 100 to 2000 keV. In the prompt gamma radiation there are very few photons with energies about or less than 100 keV and above 2 MeV. The background problem is very serious for low energies, and mostly the ratio between the number of fission photons and background improved with increasing energy. Unfortunately the counting rate for both types of radiation quite often decreases rapidly with increasing gamma-ray energy. When estimating the background in the gamma-ray energy spectra the knowledge of this variation was important. The aim of recording time-of-flight spectra as a function of gamma-ray energy was to get an idea of the over all variation of background with photon energy.

During the last 15 years some authors have discussed the life-times of the excited states of the fission fragments, but unfortunately their results have seldom been in agreement with one another. Two of the latest papers [2, 3], which also sum up the situation up to the present day, merely state that most of the gamma radiation from uranium fission is emitted within a time shorter than 50 ps. In one of Johansson's report on californium fission [1] a decay curve was reported from which a half-life of 20 ps was estimated, and then a slower component with a half-life of about 50 ps is also seen in part. These values agree well with the two slowest components seen by us.

With the collimator technique used in this experiment it is difficult to measure when the prompt gamma radiation really starts. A reasonable guess is at about $10^{-14}$ s after fission. In such a short time, however, the fragments are practically still in the foil, and it is impossible to distinguish the gamma radiation from one or the other of a pair of fragments by using our type of collimator technique. In principle it is possible to use the Doppler shift [4, 5] technique, by placing the gamma detector behind one of the fragment detectors, and measure

---

[2] Maier-Leibnitz, H., Armbruster, P. and Specht, H.J., Physics and Chemistry of Fission (International Atomic Energy Agency, Vienna, 1965), Vol. II, p. 113.

[3] Val'skii, G.V., Kaminker, D.M., Petrov, G.A. and Popeko, L.A. At. Energ. (USSR) 18 (1965) 223 (Sov. J. At. Energy 18 (1965) 279).

[4] Bowman, H.R., Thompson, S.G. and Rasmussen, J.O., Phys. Rev. Lett. 12 (1964) 195.

[5] Maier-Leibnitz, H., Schmitt, H.W. and Armbruster, P., Pysics and Chemistry of Fission (International Atomic Energy Agency, Vienna, 1965), Vol. II, p. 143.

the shift in energy of a certain gamma-ray peak when the fragment is moving in the direction to or from the gamma detector. On the other hand it is impossible to determine at which time interval after fission the respective photons have been emitted. A coincidence combination of these two techniques is not possible either, as there are several decays during the first ns of a fragment's life-time. Rough estimates of of the photon yield during different times after fission can be obtained by varying the collimator setting: a very broad one covering the foil and a few mm on both sides of it, and then selecting some narrower settings covering parts of one of the fragment's flight path. By assuming that the radiation of the fragments is isotropic it is possible to estimate the intensity of the gamma radiation during the very first instants of the fragment's life-time.

The 7 ps half-life was measured with the smallest possible collimator slit that we can use for intensity reasons at present. The value may not be necessarily correct, but contain an average over a few or even many decays. It has been assumed [1] that the prompt gamma radiation mainly consists of collective quadrupole radiation. As will be mentioned later in this report, practically all fragments emit about 1200 keV gamma-rays in this time region, and that energy corresponds well with known values for collective quadrupole radiation with this half-life. But the good correspondence between half-life and gamma-ray energy may be a consequence of the collimator used, which might happen to let through this type of radiation at this moment after fission. With increased fission rate it might be possible to get some additional details out of this fast component.

Gamma-ray energy spectra as a function of fragment mass have been recorded for which the collimator settings were chosen to select as much as possible of the three respective decays mentioned above. With the collimator set so that most of the fission gamma radiation consisted of the 7 ps component, the gamma-ray spectra looked very similar for all masses, with a broad bump around 1200 keV. With the collimator placed to let throught photons with a half-life of mostly 20 ps, there were some differences in the gamma spectra, but not much. Most of them had a bump around 700 keV. When the 50 ps component was enhanced, however, clear differences appeared between the gamma spectra. Spectra from fragments with mass numbers around 110 and above

150 had distinct peaks with energies around 250 keV, and spectra from fragments with mass numbers around 82 and 132 had bumps around 250 and 1200 keV (Fig. II.2.1.).

The fastest gamma radiation showed very little dependence on mass. The same result has been obtained from californium fission [1] and there it was discussed as being an effect originating from the high excitation energies of the fragments just after scission. When the prompt neutrons have been emitted, the fragments are still highly excited with energies well above the neutron threshold. That the following gamma emission starts above the neutron threshold is probably a consequence of the high spins of the states when the fragments have been formed. This is an effect which seems to be common for all fragments. When the first gamma emissions have taken place, one can say that the fragments change identity and become "normal" nuclei. The differences in shape between the gamma spectra of the slowest radiation mentioned above were very distinct as one goes from one mass region to another.

It is interesting to see how the decays take place in the slow time region. The soft nuclei, with mass numbers around 110 and above 150, emit many low-energy photons, which can be seen in the spectra, but also from the curve of the number of photons of energies around 200 keV as a function of fragment mass. This is a saw-tooth curve. Unfortunately we have not so far been able to estimate the background, which is considerable in this gamma-ray energy region, but the only effect it will have will be to make the difference in yields between hard and soft nuclei greater. In the raw data the background is included and measurements were also performed to enable us to subtract it. This will also be done in a further analysis.

In the mass region around 130 there are photons with energies around 250 and 1200 keV. If the 1200 keV transition is a quadrupole radiation, it should be faster, and hardly not seen with this collimator setting, at least if it is of collective nature. The 250 keV photons may be in coincidence and preceding the 1200 keV gamma-ray in a cascade. This could be an effect depending on beta-vibration in spherical nuclei where the first excited state is expected to be found between 1 and 1.5 MeV, and the second excited state a few hundred keV above the first

one and then the third excited state a few hundred keV further above. The delayed ($T_{1/2}$ = 50 ns) gamma radiation in $^{252}$Cf fission has given similar spectra [6].

The 700 keV gamma yield for a half-life of 20 ps and about 200 keV for a half-life of 50 ps corresponds well with known data for collective quadrupole radiation. If the above-mentioned result of 1200 keV for a 7 ps component is not a mere accident, the connection between half-life and gamma-ray energy is a good indication that we are dealing with collective quadrupole radiation in the prompt gamma decays.

Two reactor periods, each of almost three weeks, were devoted to the study of gamma-ray energy spectra as functions of the sum of the fragment kinetic energies. This type of measurement must be considered as preliminary, as the variation with fragment mass is not included. One short measurement, however, was done over a few days in which the total kinetic energies were recorded as a function of the mass spectrum and in coincidence with the fission gamma radiation, but the variation with gamma-ray energy was not included. Unfortunnately no three-parameter data acquisition system is available here, but these first studies will be followed by others in which a single channel analyzer will be used to select specific regions of the mass curve, and so it will be possible to get better estimates of the gamma-ray energy release as a function of fragment mass.

The first measurement was done without the lead collimator, so all prompt gamma radiation within about 2 ns was recorded. The yield of the number of photons with energies less than about 2 MeV as a function of the total kinetic energy is a smooth function, decreasing slowly with total kinetic energy (Fig. III. 2. 2. ). The general trend of the yield curve does not change when more limited gamma energy regions are studied. This means that the total amount of energy released as a function of the sum of the kinetic energies varies in the same way. The second measurement was done with the collimator placed so that it just "shadowed" the foil and the very first gamma radiation, but let through the main part of the prompt gamma radiation. The yield of the number of photons with energies less than about 2 MeV as a function of the total kinetic energy was very similar to the first case.

---

[6] Johansson, S. A. E. , Nucl. Phys. 64 (1965) 147.

The fissioning nucleus contains a given amount of energy which will be shared between the kinetic and the excitation energies of the fragments. The total kinetic energy of the fragments in uranium fission as a function of the mass number has, as is well known, low values for symmetric and very asymmetric fission. In this case it is enough to study the variation around the heavy mass peak. The function rises quickly with mass number and has a maximum around mass number 132. Consider then the prompt neutron yield as a function of the total kinetic energies of the fragments. For uranium [7] and californium [8] fission the neutron yield curves have similar shapes to those obtained for the prompt gamma radiation in this experiment. For the yield of the prompt gamma radiation as a function of the total kinetic energy the result is reasonable from the energy point of view, because it says that, as more energy is added to the kinetic energies, less energy is left for the fragment deexcitation, leading to decays by prompt neutrons and gammas.

[7] Maslin, E. E., Rodgers, A. L. and Core, W. G. F., Phys. Rev. 164 (1967) 1520.

[8] Bowman, H. R., Milton, J. C. D., Thompson, S. G. and Swiatecki, W., Phys. Rev. 129 (1963) 2133.

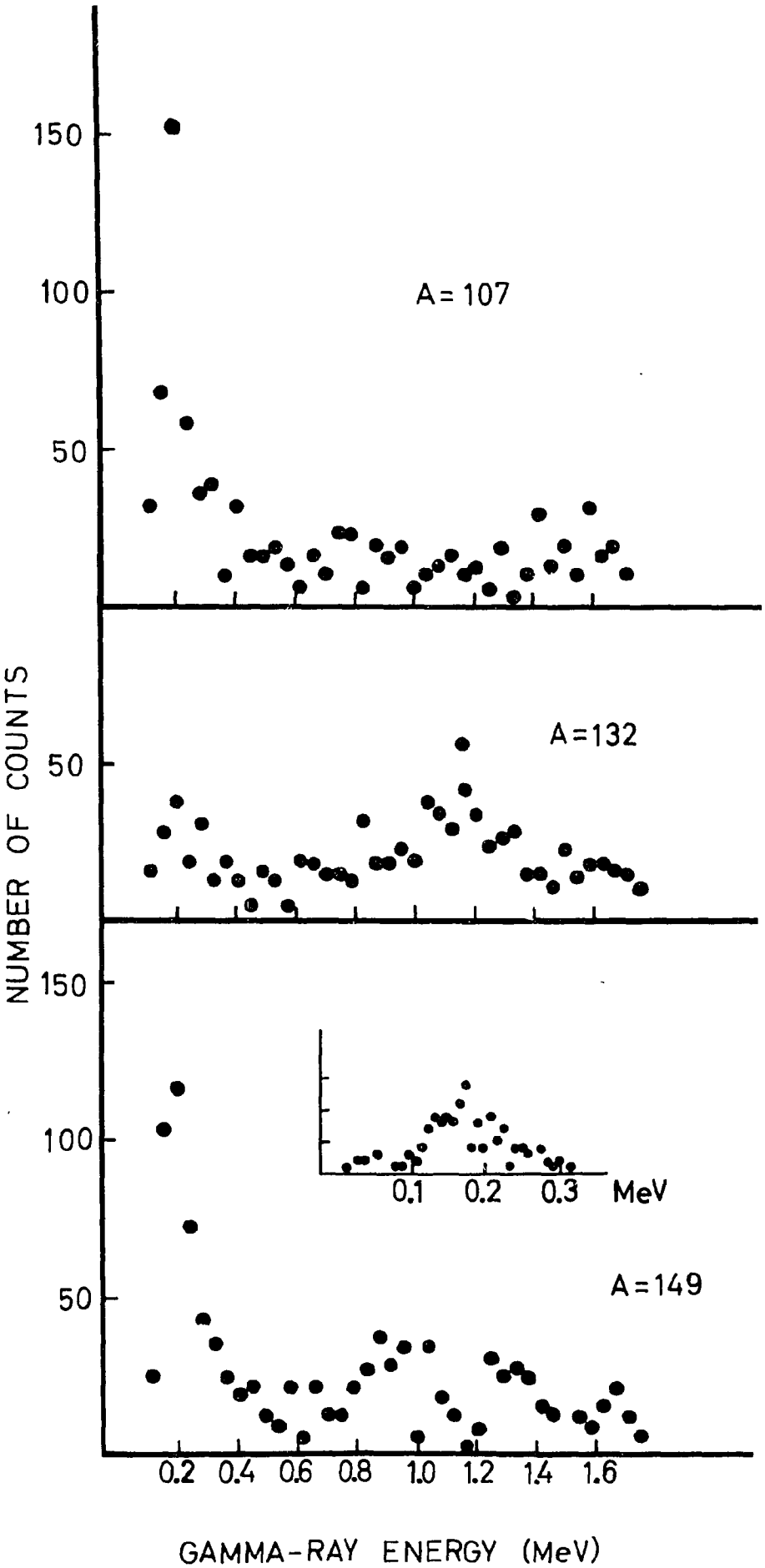


Fig. III. 2. 1. Gamma-ray energy spectra associated with the 50 ps half-life for three different mass regions.

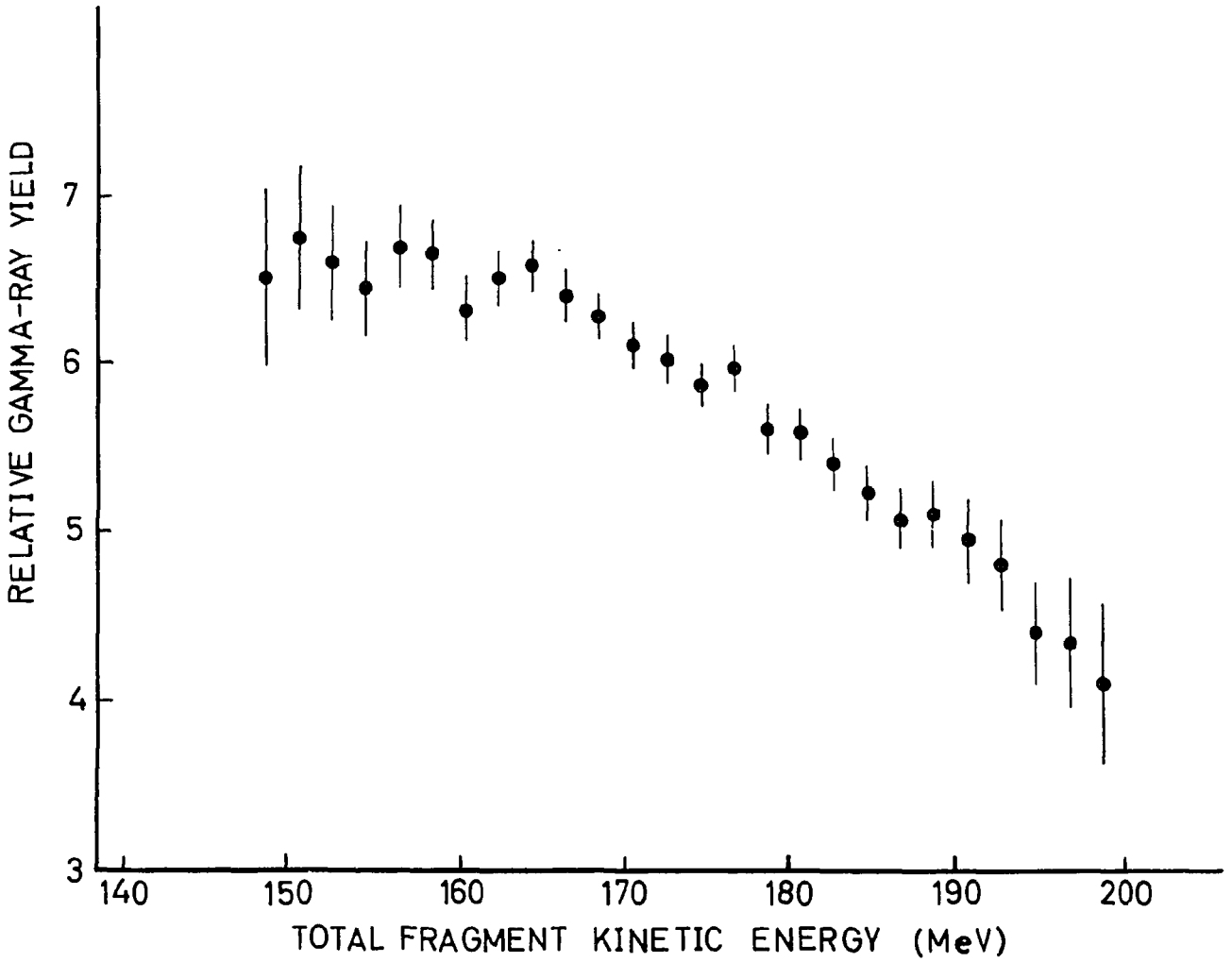


Fig. III.2.2. Relative gamma-ray yield as a function of the total fragment kinetic energy.

# IV. THEORETICAL PHYSICS

## IV. 1. LEVEL DENSITIES OF SPHERICAL NUCLEI FROM EXACT COUNTING OF SHELL MODEL STATED

J. Eriksson and S. Jägare*

The standard way to treat the problem of nuclear level densities [1-3] is to picture the nucleus as a mixture of two degenerate Fermi gases of independent neutrons and protons, respectively. In these calculations the following approximations are usually employed:

(i) The replacement of the single-particle level density g by a smooth function,

(ii) the neglect of terms depending on derivatives of g and putting g equal to its value at the Fermi level,

(iii) the use of the saddle-point approximation in evaluating the Laplace transform defining the level density.

It is clear that points (i) and (ii) disregard all effects of nuclear shells. Some simple semi-empirical models have been introduced and parametrized in order to study these effects and effects orginating from correlations (especially the pairing correlation) among the nucleons. From such studies, see especially the review by Ericson [1], and experimental evidence [3] it is found that the level densities, even at high excitation energies, are affected in a major way by nuclear shell structure and pairing effects. Despite the usually rather good agreement between calculated and observed level densities it is not clear that the main physical effects are properly included in the existing models, and the present knowledge about nuclear level densities must be considered to be scanty.

In order to study especially the effects of nuclear shells on level densities of spherical nuclei we have undertaken the problem of exact numerical counting of shell model states in a spherical potential. In this way we avoid any assumptions and approximations concerning single-particle level densities and mathematical methods. The single-particle shell model levels are subjected to a standard BCS calculation and the

[1] T. Ericsson, Adv. Phys 9 (1960) 425

[2] A. Gilbert and A G.W. Cameron, Can. J. Phys. 43 (1965) 1446

[3] A. Bohr and B. Mottelson, Nuclear Structure, Vol. I, chapter 2

* Research Institute for Physics, Stockholm

resulting quasi particle energies are then used as input in a level counting computer program and the quantities

$$\rho(E, I), \quad \rho(E) = \sum_I \rho(E, I), \quad W(E) = \sum_I (2I + 1)\, \rho(E, I)$$

are calculated. Here $\rho(E, I)$ is the density (in $MeV^{-1}$) of levels of given angular momentum I (both parities included) at an excitation energy E above the ground state. The observable level density is $\rho(E)$ and $W(E)$ is called the total level density. These quantities are then compared to the extensively used analogous quantities [2]

$$\rho_{FG}(U, I) = f(U, I;\, a, U_o,\, \sigma),$$

$$\rho_{FG}(U) = h(U;\, a,\, U_o,\, \sigma),$$

$$W_{FG}(U) = \sqrt{2\pi}\, \sigma\, h(U;\, a,\, U_o,\, \sigma),$$

obtained from the Fermi gas model by use of the approximations (i)--(iii) above. The excitation energy U in this model is related to E by $U = E - U_o$, a is the parameter usually called the level density parameter and $\sigma(E)$ is the spin cut-off parameter.

Calculations for different magic region nuclei are in progress. Available preliminary results of $\rho(E)$ and $\rho_{FG}(U)$ from best fits are shown in Fig. IV.1.1. for the case of $^{208}Pb$ and $^{202}Hg$. We observe significant shell structure oscillations for the $^{208}Pb$. These are caused by inferior energetic overlap of the level densities originating from the different neutron plus proton total quasiparticle numbers. Thus details in the variation of the level densities usually should be understood in terms of the specific single-particle level scheme. Despite the low energy data scattering we observe the strong exponential increase of the level density $\rho(E)$ at higher energies, in agreement with the Fermi gas model prediction.

Examples of the spin cut-off parameters $\sigma(E)$ of $^{208}Pb$ and $^{202}Hg$ are given in the lower part of Fig. IV.1.1. showing that their predicted $U^{1/4}$ dependence, which we parametrize as

$$\sigma(E) = q_\sigma\, (E - U_o)^{1/4}, \quad E \geq U_o$$

is well reproduced. Preliminary results for the energy independent parameters a, $U_o$ and $q_\sigma$, as obtained from best fits of the Fermi gas relations to the calculated level density functions, are given for $^{208}Pb$ isotopes and isotones in Table 1. The magnitudes of $\sigma$ are all some 20 % larger than earlier values. This probably means that higher spin values are often missed in experiments. We also observe that the magnitude of the parameter a is by 10 - 20 % smaller than values obtained from the analysis of experimental data. In such comparisons a constant pairing energy is the only contribution to the $U_o$ while in our calculations $U_o$ involves both shell and pairing effects, the latter being comparatively small in magic nuclei regions. Sufficiently far from closed shells we expect the increasing pairing contribution to $U_o$ to become dominant, thus also increasing the a-values.

Table 1. Values of the parameters a, $U_o$ and $q_\sigma$ from the best fits of the Fermi gas.

| 126 Neutrons | | | | 82 Protons | | | |
|---|---|---|---|---|---|---|---|
| Protons | a | $U_o$ | $q_\sigma$ | Neutrons | a | $U_o$ | $q_\sigma$ |
| 77 | 13.71 | 2.85 | 3.93 | 121 | 13.11 | 2.90 | 3.85 |
| 78 | 13.61 | 3.08 | 3.88 | 122 | 13.36 | 2 64 | 3.83 |
| 79 | 12.79 | 2.47 | 3.75 | 123 | 13.14 | 2 80 | 3.79 |
| 80 | 11.95 | 3.05 | 3.65 | 124 | 12.20 | 3.55 | 3.75 |
| 81 | 12.03 | 3.72 | 3 71 | 125 | 11.63 | 3.46 | 3.69 |
| 82 | 12.84 | 5.53 | 3.89 | 126 | - | - | - |
| 83 | 12.89 | 3.55 | 4.01 | 127 | 12.42 | 3.27 | 3.96 |
| 84 | 13.01 | 2.58 | 4.11 | 128 | 12.28 | 2.16 | 4.06 |
| 85 | 12 54 | 0.12 | 4.13 | 129 | 12.35 | 0.09 | 4.15 |
| 86 | 13.90 | 1.54 | 4.35 | 130 | 13.31 | 1.40 | 4.31 |
| 87 | 14.02 | -0.16 | 4.43 | 131 | 13.77 | -0.19 | 4.46 |

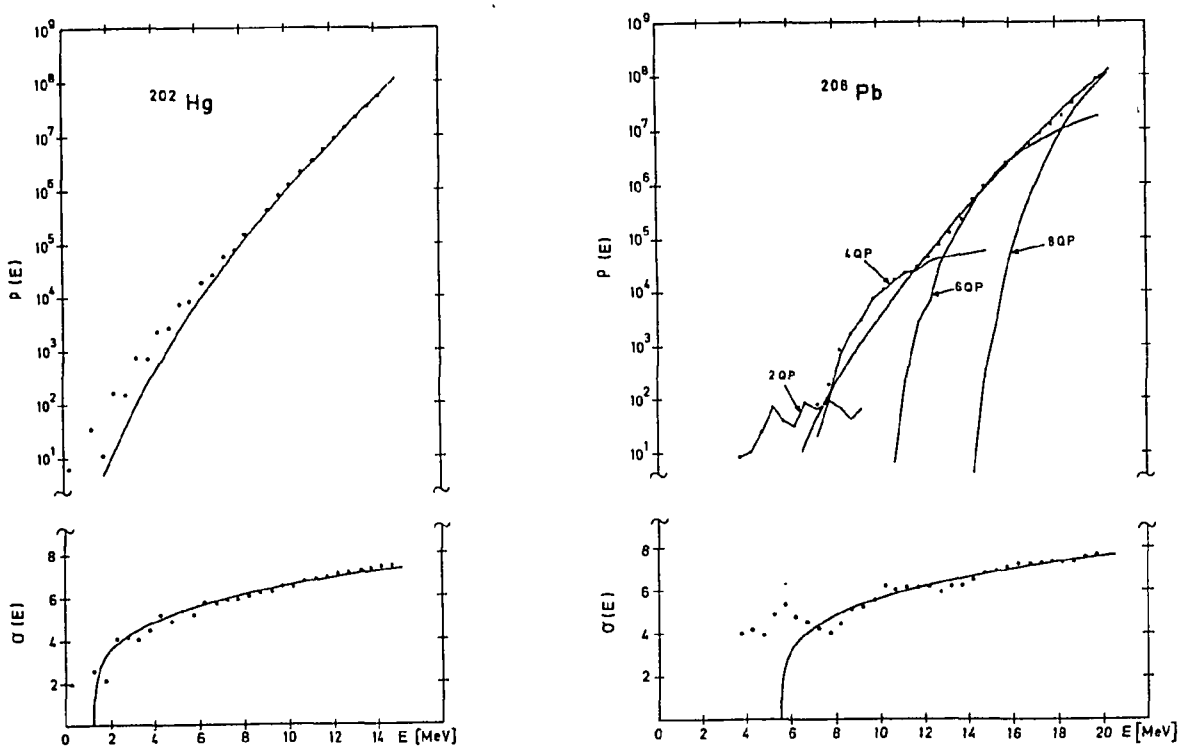


Fig. IV. 1. 1. The energy dependence of the level density ρ(E) and the spin cutoff parameter σ(E) for $^{208}$Pb and $^{202}$Hg. The points give the shell model prediction and the full lines the best Fermi gas fits. The total numbers of the different quasiparticle (QP) contributions to the total level density ρ(E) of $^{208}$Pb are given.

# IV.2. A NON-LOCAL POTENTIAL APPROACH IN THE RELATIVISTIC NUCLEON-NUCLEON SCATTERING

J. Eriksson

The momentum space factor m/E represents to a considerable extent the momentum dependence of the relativistic single particle exchange amplitudes in the elastic N-N scattering. Starting from the non-locality derived from m/E, as proposed by Wong [1], a computationally feasible method of integrating the Schrödinger equation is given.

It may for particular potentials $V(r, k^2)$ be possible, instead of the usual momentum square expansion

$$V(r,k^2) = \sum_{i=o}^{\infty} V_i(r)\, k^{2i},$$

to make a product decomposition

$$V(r,k^2) = N(k^2)\, U(r,k^2)$$

with the reduced one-body momentum k and r the radial coordinate. In the N-N scattering through intermediate meson forces, to a good approximation a factor $N(k^2)$ may be separated off. This $N(k^2)$ operates on some function $\chi(\underline{r})$ as a non-local integral in the configuration space

$$N(k^2)\, \chi(\underline{r}) = \int N(|\underline{r}-\underline{r}'|)\, \chi(\underline{r}')\, d\underline{r}'$$

The Fourier transform of $N(|\underline{r}-\underline{r}'|)$ is identified as the momentum space factor m/E. Since the non-local kernel is

$$N(|\underline{r}-\underline{r}'|) = K_1(|\underline{r}-\underline{r}'|)/2\pi^2 |r-r'|$$

with $K_1$ a modified Bessel function, an addition theorem [2] of these modified Bessel functions $I_\nu$ and $K_\nu$ is used to express the non-local kernel as an expansion in spherical coordinates. Thus the operator

---

[1] D.Y. Wong, Nucl. Phys. 55 (1964) 212.

[2] G.N Watson, Theory of Bessel Functions, (Cambridge University Press, New York), 2nd ed. (1958) 365.

$N(k^2)$ takes the form

$$rN(k^2)\left[\frac{\varphi_\ell(r)}{r}\ Y_\ell^m(\Omega)\right] = Y_\ell^m(\Omega)\ \sum_{i=0}^{\infty} q_{i\ell}\ F_{2i+\ell+1}(r;\ \varphi_\ell)$$

with

$$F_\nu(r;\ \varphi_\ell) = K_\nu(r) \int_0^r I_\nu(\acute{r})\ \varphi_\ell(\acute{r})\ d\acute{r} + I_\nu(r) \int_r^\infty K_\nu(\acute{r})\ \varphi_\ell(\acute{r})\ d\acute{r}$$

when working on some function $\varphi_\ell(r)\ Y_\ell^m(\Omega)$. Here $\varphi_\ell(r) = U(r, k^2) \cdot u_\ell(r)$ and $u_\ell(r)$ is a partial wave in the common notation and the factors $q_{i\ell} \to 4/\pi$ for $i \to \infty$. It is found that $N(k^2)$ is defined for a class of functions with $\varphi_\ell(r) = 0[\ln(r^{-1})]$ for $r \to +0$ and, this is particularly nice, the rate of convergence in i of the expansion is so fast that just the three lowest terms with a simply estimated rest term hold good. Numerical procedures for economical use of a computer have been worked out for obtaining the solutions of the integro-differential Schrödinger equation.

This work is in progress of publication.

# IV.3. A SLOW NEUTRON SCATTERING ROUTINE FROM THE GAS MODEL

J. Eriksson

The Monte Carlo method, commonly used in computing the neutron energy and density distributions in exceptional geometries by tracing individual neutron paths, to a large extent consumes computer time in the scattering routine itself. Starting from a scattering formalism given by Zemach and Glauber [1] and assuming a Maxwellian energy distribution of the scattering medium, a simplified scattering routine was obtained. Any transformation to or from the centre-of-mass system thereby becomes suppressed.

With the neutron's initial velocity v, its final velocity $\acute{v}$ and the scattering cosine $\mu$, the main problem is to sample a couple $(\acute{v}, \mu)$. From the closed expression of the laboratory system differential cross section it proved possible to find a transformation from the $(\acute{v}, \mu)$ to an auxilary couple $(p, q)$ with the sampling density $p \exp(-q^2)$ being factorized. Further, the sampling domain $R(p, q)$

$$R(p,q) = \begin{cases} 0 \le p < \infty \\ \left(\frac{1+\lambda}{2} p - 1\right) x^* \le q \le \left(\frac{1+\lambda}{2} p + 1\right) x^* \end{cases}$$

is entirely bound by straight lines. Here $\lambda$ is the scattered neutron to the scatterer mass quotient and $x^*$ is the initial velocity v given in thermal units of the scattering system. Once $(p, q)$ is given, the inverse transformation

$$Z = \sqrt{\frac{2pq}{x^*} - \lambda p^2 + 1}$$

$$\mu = \frac{1 + Z^2 - p^2}{2Z}$$

with $\acute{v} = Zv$ gives the scattering parameter $(\acute{v}, \mu)$ in the laboratory system.

---

[1] A. C. Zemach and R. J. Glauber, Phys. Rev. 101 (1956) 118

# V. VAN DE GRAAFF ACCELERATOR

## V.1. ACCELERATOR PERFORMANCE

P. Tykesson

The Van de Graaff accelerator has been used with protons, deuterons and helium ions, both with DC beams and pulsed beams. The accelerator was run in alternately two and three shifts for 5 days per week and the calculated total time available for experiments was 3336 hours 3224 hours of which were used by the scientists and 110 hours were required for unforeseen maintenance.

The distribution of the available machine time for experiments with the accelerator performed by physicists from various institutes is shown in Table I and of different experimental branches in Table II.

Table I

| | |
|---|---|
| AB Atomenergi | 77.7 % |
| Research Institute of National Defence (FOA) | 11.9 % |
| Chalmers University of Technology | 8.9 % |
| University of Aarhus, Denmark | 1.5 % |

Table II

| | |
|---|---|
| Nuclear physics | 17.2 % |
| Neutron physics | 67.8 % |
| Solid state physics | 13.9 % |
| Irradiations | 1.1 % |

The number of normal breaks for maintenance of the machine have been four during the year, each generally consisting of one week.

The accelerator has been equipped with the klystron bunching system for about one and a half year and the system has been working under ordinary working conditions for about 3000 hours. It has proved the expected performance with regard to ion beam intensity

and time compression. At the beginning there were some problems caused by metallic contamination of the insulators of the bunching tube, but after shielding the bunching system has proved very reliable.

## V.2. ION SOURCE IMPROVEMENTS AND TEST RESULTS

P. Tykesson

The continued development of the accelerator is being directed to the possibilities of increasing the beam intensity with preserved duration of the bursts of about 1 ns. By changing the bunching frequency from 15 to 10 MHz more of the beam can be utilized in forming the ion burst. The variations of the peak current gain and the bunched pulse width when changing the machine voltage are shown in Figs. V.2.1. and V.2.2. respectively. The figures also illustrates the influence of the width of the chopped pulse.

The ion energy spread originating from the ion source causes a debunching effect and is an important factor for an optimal short pulse operation of klystron bunching. The energy spread can vary from a few electron volts to 1 keV depending on the type of source and mode of source operation. Two different types of R.F. sources, both of HVEC manufacture, have been tested in respect to the energy spread in the extracted beam. The main difference between the two sources is the design of the anodes. The first type (C-SO-164) has a small tungsten anode hidden from the discharge by a pyrex shield and the other one (C-SO-173) has an anode cap of aluminium in direct contact with the discharge. The R.F. oscillator used in the tests operates at a frequency of 145 MHz. The energy spread was measured with the retarding field analyzing method. Fig. V.2.3 shows the energy spread full width at half height at two gas pressures as function of the magnet coil current. The source type C-SO-164 seems to have a lower energy spread than that of type C-SO-173. No attempts have been made to optimize the R.F. power, the extraction voltage or the location of the magnet coil.

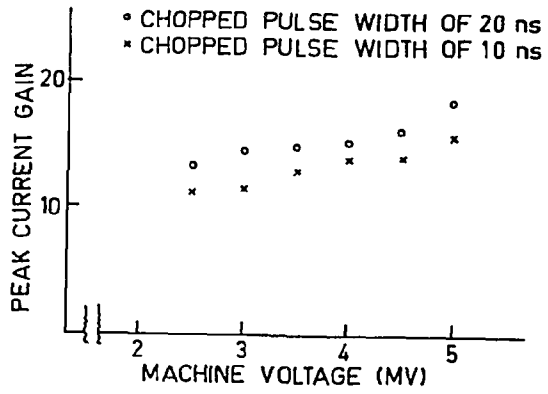


Fig. V.2.1. The peak current gain for different settings of the machine voltage and two different widths of the chopped pulse.

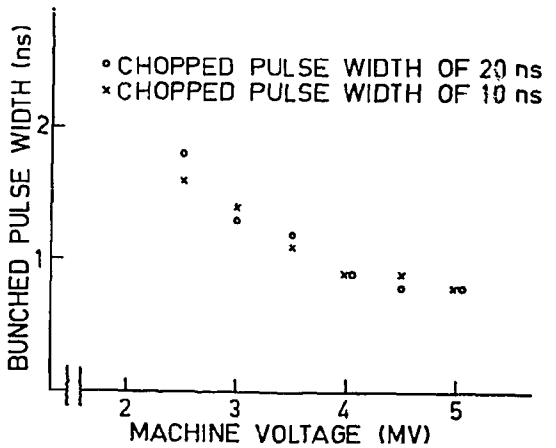


Fig. V.2.2. The bunched pulse width for different settings of the machine voltage and two different widths of the chopped pulse.

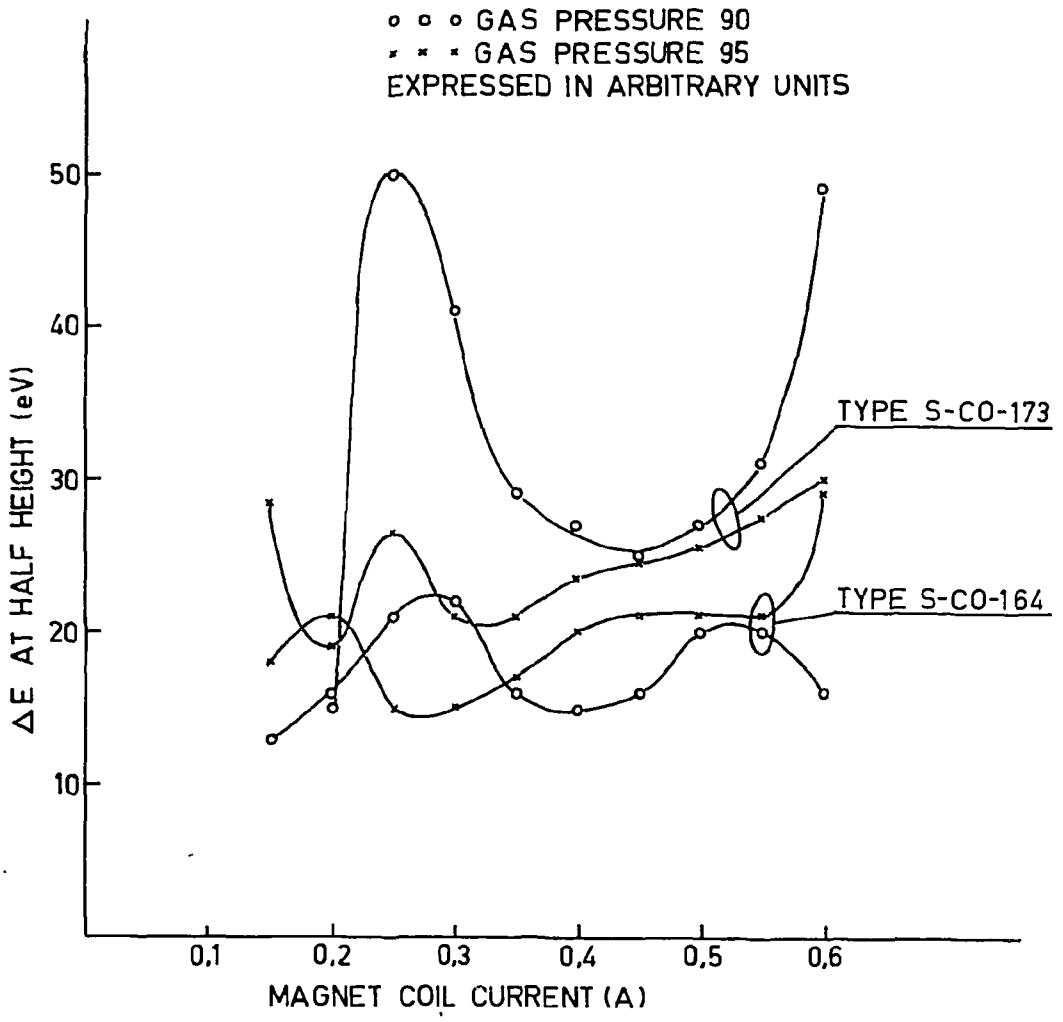


Fig. V.2.3. The energy spread for two different ion sources as function of the coil current.

# VI. CHANNELING STUDIES

Experiments carried out in recent years have shown that, when an energetic charged particle enters a monocrystalline target within a certain critical angle of either a low-index direction or a low-index plane, the particle will be steered by successive small angle scattering events and is therefore prevented from undergoing violent collisions with individual lattice atoms. Therefore these particles will show anomalous penetrations and energy-loss rates. Also atomic and nuclear reaction yields are orientation dependent, i.e. the yield of head-on collisions (e.g. Rutherford scattering, nuclear reactions, and x-ray production) will be drastically reduced. This steering process - usually referred to as particle channeling - has been demonstrated with a wide variety of ions, ion energies and target materials.

When measurements in the channeling field started at the Studsvik Van de Graaff laboratory nearly all reported work had been on monatomic crystals. Therefore it was decided to study more complex crystals and as a first step to study diatomic crystals.

Beside the possibility of studying the fundamental aspects of channeling in a complex system, the use of diatomic crystals will also give information of interest for experiments like looking for foreign atoms in the lattice. Such measurements are of interest, for example, in the reactor technology.

## VI. 1. CHANNELING STUDIES IN SINGLE CRYSTALS OF CALCIUM FLUORIDE

R. Hellborg

Single crystals of $CaF_2$ have been bombarded with high energy (0.6 - 4.0 MeV) protons and helium ions to study the channeling effect. The steering properties of each sublattice (Ca and F resp.) were measured independently. To study the interaction with the Ca-atoms Rutherford scattered ions in the back direction were detected. To study the interaction of the ions with the F-sublattice the resonant nuclear reaction

$F^{19}$ (p, $\alpha\gamma$) $O^{16}$ was used. The critical angle and the minumum yield have been studied with variation of different parameters such as species of ion, energy of ion, scattering depth in the crystal, interaction with the two sublattices and temperature of the crystal.

Along those directions where the fluorine and calcium atoms lie on separate atomic rows or planes, the two processes exhibit completely different orientation dependencies. On the other hand, along directions where both atomic species lie on the same row or plane, the orientation dependencies of the two processes are identical. The observed values of the critical angles are 20 - 30 % smaller than theoretical predictions even when lattice vibrations are included in the theoretical calculation.

The orientation dependence of the yield of elastic scattering and nuclear reaction in a zone close to the crystal surface is illustrated in Fig. VI. 1.1. Preliminary results will be found in [1 ], [2].

## VI. 2. THE ENERGY LOSS OF CHANNELED PROTONS DETERMINED IN AN INDIRECT WAY

R. Hellborg

Particles steered by successive small angle scattering events are prevented from undergoing violent collisions with individual lattice atoms. And therefore these particles are moving in a low nuclear and electron density. And therefore they will show a lower energy-loss rate than particles moving in a random direction (i. e. an amorf target).

From some calculations in the above reported measurements on $CaF_2$ single crystals, it is necessary to know the energy-loss rate of the incoming ions along different axes. The common way to measure the energy-loss is by use of thin crystals. For lack of thin crystals the energy-loss rate has been measured in an indirect way. The energy distribution of detected alpha particles from the resonant nuclear reaction $F^{19}$ (p, $\alpha_o$) $O^{16}$ induced by channeled protons in a single crystal of $CaF_2$ will give information about the proton energy-loss rate in the channel. Preliminary calculations from experimental investigations give $\alpha$=0. 3-0. 4; where $\alpha$ is the ratio between energy-loss rate in channel and in random direction.

---

[1 ] R. Hellborg, Critical angles for protons channeled to various depths in a $CaF_2$ single-crystal, AE-FFS-18.

[2 ] R. Hellborg, Channeling studies in a diatomic single crystal, AE-FF-93.

## VI. 3. CHANNELING MEASUREMENTS WITH SINGLE CRYSTALS OF $TiO_2$ AND $H_2O$*

R. Hellborg

In earlier experiments with diatomic single crystals a systematic discrepancy has been found between experimental and calculated values of the critical angles. Even when the thermal vibration of the lattice is included in the theoretical calculation, the experimental values are typically 25 % lower than calculated values. In bcc and fcc monatomic crystals the agreement is within 10 %. Therefore som systematic investigations documenting this difference, will perhaps give material for a better theoretical model.

To go on with the channeling measurements in diatomic crystals we have selected single crystals of $TiO_2$. This crystal has a configuration of its atoms attractive for channeling experiments. Preliminary experiments show that this is a suitable crystal.

At what temperature do ice crystals begin to break up and melt? This is an interesting question which perhaps can be answered by the use of the channeling technique. The condition of the crystal at temperatures close to zero degree will be frozen in by quick quenching the crystal to a very low temperature where the measurement is easier to make. The measurements are made with a goniometer which can be cooled down to liquid nitrogen temperature. The experimental technique has been improved and preliminary measurements have been made.

In the ice crystal experiments the Department of Physical Chemistry at the Royal Institute of Technology has taken part by providing the ice single crystals.

## VI. 4. STRUCTURE CHANGES DURING AGING IN Al-Cu (4%) SINGLE CRYSTALS

R. Hellborg and U. Bergenlid**

The hardening of alloys by aging is of great industrial importance and unusual scientific interest. The changes of physical properties, which are exceedingly varied and complex, have been the subject of

---

* In collaboration with the Solid State Group at Research Institute for Physics, Stockholm.

**

many investigations. For an alloy to age-harden it must have a decreasing solubility with decreasing temperature, so that when the alloy is given a solution heat treatment and then a quench to a lower temperature, it will be supersaturated with respect to one or more dissolved elements and will undergo structural changes.

In many alloys the precipitation process consist of the sequential reactions: supersaturated solid solution → one or more transition states → saturated solution → equilibrium precipitate. The initial and final states correspond to the phases of the equilibrium phase diagram. The transition states are often less easily identified.

During aging of single crystals of Al-Cu (4%) alloy thin plates of $CuAl_2$ with a diameter of some thousand ångström but only some tenth atomic layers thick precipitate. At first the precipitations are coherent with the Al matrix but after more aging they will grow and the tensions will be so big that dislocations appear and the coherence disappear in part. By use of the channeling effect it is possible to study the coherence during this transition state.

After annealing and quenching the crystals (as a result of which nearly all copper atoms will be on lattice position - supersaturated solid solution), the crystals have been aged at different high temperatures giving different transition states. By use of the channeling technique, the number of copper atoms not on lattice position have been measured for these different transition states. Two annealing temperatures (200 and 300°C) have been used and an aging time between 15 minutes and 16 hours, that is states from supersaturated solid solution to the equilibrium precipitate have been studies. These measurements will now be correlated with electron-microscopic studies.

## VI. 5. CHANNELING IN $BaF_2$

R. Hellborg

Some of the results from the investigation of the $CaF_2$ single crystal show that more measurements with this kind of diatomic crystals would be of interest. For these measurements crystals of $BaF_2$ have been chosen. Still the reaction $F^{19}(p, \alpha\gamma)O^{16}$ can be used in studying the F-sublattice.

For $BaF_2$ the amplitudes of the thermal vibrations for the two species of atoms are known in a big temperature interval.

Measurements of the critical angle and minimum yield have been made at temperatures from room temperature down to -190°C. With a new goniometer now under installation it will be possible to heat the crystal and make measurements at crystal temperatures of several hundred degrees celsius.

Figure VI. 5. 1 shows experimental values of the critical angle $\Psi_{1/2}$ for two axies in $BaF_2$, <111> and <110>. The proton energy was 873 keV. $\Psi_{1/2}$ is given as a function of depth in the crystal for both the elastic scattering and the nuclear reaction yield. The depth in the crystal is given as the inelastic energy losses in the crystal (1 μ corresponds to 30 - 40 keV).

For <111> the measurements give the same value of the critical angle for both processes. This is to be expected since along the <111> direction all rows are identical. Along the <110> direction the critical angle for the nuclear reaction process is narrower than that for the elastic scattering process since Ba and F atoms lie on separate rows. Therefore the two processes need not have the same angular dependence along <110>.

As is well known critical angles exhibit depth effects. Along <111>, $\Psi_{1/2}$ decreases with increasing depth due to dechanneling effects. The elastic scattering and the nuclear reaction processes give the same $\Psi_{1/2}$ value and show the same depth dependence as expected. Along the <110> direction the interaction with the F-rows shows only a slight depth dependence, the interaction with the Ba-rows, however, shows a drastic change with depth close to the surface.

In figure VI. 5. 1. we also see some measurements at a low temperature (-190°C). The critical angle seems to change to a value 15 - 30 % larger than at room temperature for both axies investigated when the temperature is lowered. The change is about the same for the interaction both with Ba-sublattice and F-sublattice. And we can see no difference in the depth dependence at the two temperatures (20°C and -190°C).

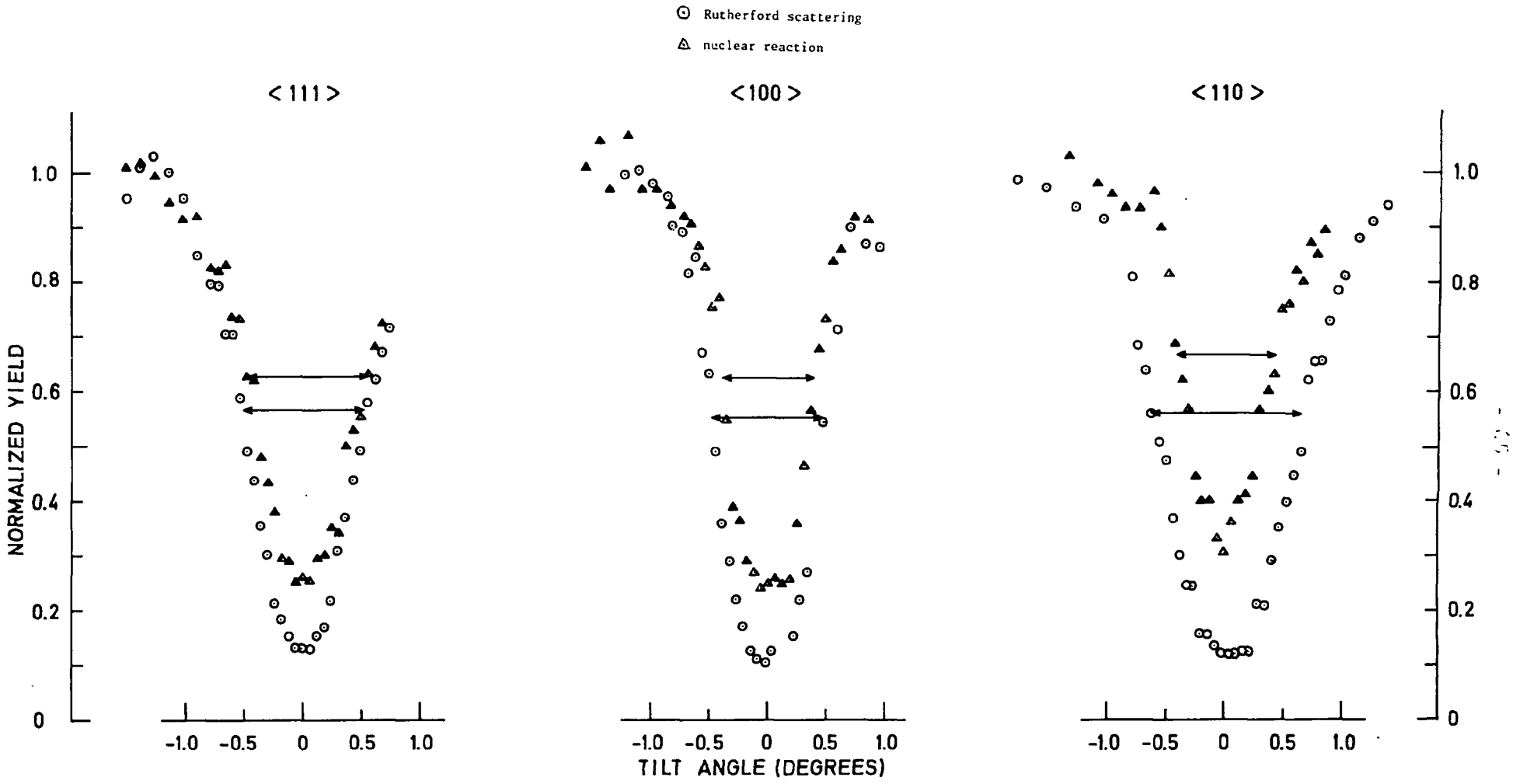


VI.1.1. Orientation dependence of the yield of Rutherford scattering (o) and of nuclear reaction (Δ) in a $CaF_2$ single crystal. The zone of interaction is close to the crystal surface. Proton energy 873 keV.

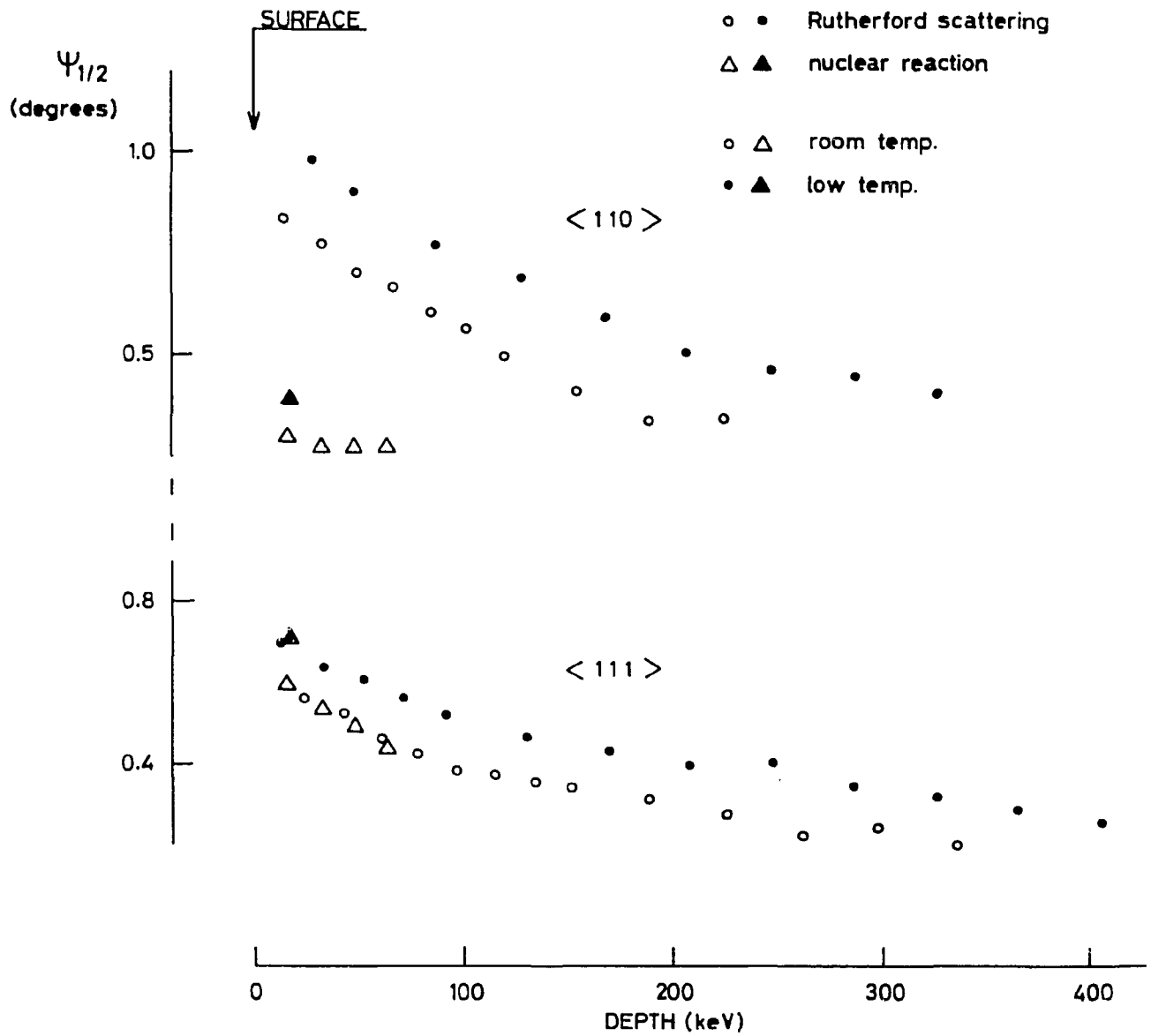


VI. 5. 1. The critical angle, as a function of depth in the crystal, for the elastic scattering and the nuclear reaction yield. The measurements are for two axies (<111> and <110>) and two temperatures (20° and -190°C) in a $BaF_2$ single crystal.

# VII. STAFF

| | | |
|---|---|---|
| T. Wiedling | In charge | |
| M-L Olsson (Miss) | Secretary | |
| H. Albinsson | Attached | Chalmers University of Technology |
| E. Almén | | |
| L. Anevi | | Until June 30, 1969 |
| V. Berg | Attached | University of Stockholm |
| S. Beshai | | |
| J. Eriksson | | |
| L. Eriksson | | |
| M. Etemad | Attached | Tehran University Nuclear Centre, TEHRAN, Iran |
| R. Hellborg | | |
| J. Higbie | | Until June 30, 1969 |
| B. Holmqvist | | |
| Å. Höglund | Attached | University of Stockholm |
| S. Johansson | | Until June 30, 1969 |
| R. Johnson | | |
| B. Jonsson | | |
| L. Larsson | | |
| T. Larsson | | |
| L. Lindow | | Until June 30, 1969 |
| G. Lodin | | Until June 30, 1969 |
| S. Malmskog | | |
| L. Nilsson | | |
| S. Nizamuddin | Attached | Atomic Energy Centre, Ramna, DACCA, East Pakistan |
| L. Norell | | |
| M. Salama | Attached | Atomic Energy Establishment Cairo, U.A.R., Egypt Until August 28, 1969 |
| P. Tykesson | | |

# VIII. REPORTS AND PUBLICATIONS

## REPORTS

Albinsson, H.
The Physics and Chemistry of Fission. Notes from the IAEA Symp., Vienna 28.7 - 1.8.1969.
1969, AB Atomenergi, Sweden
(Internal report FN-3)(In Swedish).

Albinsson, H. and Lindow, L.
Prompt Gamma-Rays from Thermal Neutron Induced Fission of $U^{235}$,
The Second Symposium on the Physics and Chemistry of Fission, IAEA, Vienna 28 July - 1 August, 1969.
(SM-122/40).

Benzi, V. et al.
A Non-Spherical Optical Model Analysis of Elastic Neutron Scattering from Tantalum.
1968, AB Atomenergi, Sweden
(Internat report FFN-94).

Bergqvist, I., Lundberg, B. and Nilsson L.
High-Energy Gamma-Ray Transitions from MeV Neutron Capture in $^{206}Pb$. Contribution to International Symp. on Neutron Capture Gamma-Ray Spectroscopy, Studsvik 11 - 15 Aug. 1969
Göteborg 1969.

Higbie, J.
Gamma Radiation from Fission Fragments Experimental Apparatus - Mass Spectrum Resolution 1969
(AE-367).

Holmqvist, B. et al.
Neutron Elastic Scattering Cross Sections of Iron and Zinc in the Energy Region 2.5 to 8.1 MeV. 1968
(AE-337).

Holmqvist, B. and Wiedling, T.
Neutron Elastic Scattering Cross Sections Experimental Data and Optical Model Cross Section Calculations. 1969
(AE-366).

Holmqvist, B. et al.
A Study of Deformation Effects by Fast Neutron Elastic Scattering.
1969, AB Atomenergi, Sweden
(Internal report FN-2).

Holmqvist, B. et al.
Fast Neutron Elastic and Inelastic Scattering of Vanadium. 1969
(AE-375).

Höjeberg, M. and Malmskog, S. G.
Transition Probabilities in the $1/2^+$ (631) Band in $^{235}U$. 1969
(AE-371).

Lindow, L. and Albinsson, H.
A Program Package for a Small Computer
1969, AB Atomenergi, Sweden
(Internal report FFN-100).

Lodin, G. et al.
An Optical Model Study of Elastic Neutron Scattering from Iron and Zinc
1968, AB Atomenergi, Sweden
(Internal report FFN-93).

Lodin, G. and Nilsson, L.
The $^{16}O$(d, n) $^{17}F$ Reaction in the Energy Range 2.5 to 5.5 MeV
1969, AB Atomenergi, Sweden
(Internal report FFN-98).

Höjeberg, M. and Malmskog, S. G.
A Half-Life Measurement of the 343.4 keV Level in $^{175}Lu$. 1969
(AE-361).

Malmskog, S.G. and Berg. V.
Absolute Transition Rates in $^{188}Ir$. 1969
(AE-370).

Malmskog, S.G., Höjeberg, M. and Berg, V.
On Low Energy Levels in $^{185}W$. 1969
(AE-349).

Malmskog, S.G.
(n, $\gamma$)-Cross Section Measurements in Harwell during the Autumn 1968
1969, AB Atomenergi, Sweden
(Internal report FFN-97)(In Swedish).

Nilsson, L. and Erlandsson, B.
A Study of the $^{50}Cr$(d, n) $^{51}Mn$ and $^{54}Fe$(d, n) $^{55}Co$ Reactions
1969, AB Atomenergi, Sweden
(Internal report FN-4).

Tykesson, P. and Wiedling, T.
Klystron Bunching of Ion Bursts, Contribution to the Conference "Tillämpad fysik och biofysik", Stockholm, June 4 - 6 1969.

## PUBLICATIONS

Berg, V. and Malmskog, S.G.
Transition Rates in $^{161}Dy$,
Nuclear Physics A135 (1969) 401.

Bergqvist, I. et al.
Radiative Capture in Nickel and Bismuth of Neutrons in the MeV Region,
Nuclear Physics A120 (1968) 161.

Holmqvist, B. and Wiedling, T.
Nuclear Mass Distribution Radii from Elastic Neutron Scattering,
Physics Letters 27B (1968) 411.

Holmqvist, B.
A Systematic Study of Fast Neutron Elastic Scattering in the Energy Region 1.5 to 8.1 MeV,
Arkiv Fysik 38 (1968) 403.

Höjeberg, M. and Malmskog, S.G.
A Half-Life Measurement of the 343.4 keV Level in $^{175}$Lu,
Nuclear Physics A134 (1969) 77.

Höjeberg, M. and Malmskog, S.G.
Half-Life Measurements of Levels in $^{75}$As,
Nuclear Physics A133 (1969) 691.

Malmskog, S.G. and Bäcklin, A.
The Decay of $^{191}$Os,
Arkiv Fysik 39 (1969) 411.

Nauclér, L. et al.
Gamma-Ray Spectra from (d, pγ) Reactions in $^{58,60}$Ni and $^{63,65}$Cu,
Nuclear Physics A122 (1968) 113.

## IN COURSE OF PUBLICATION

Berg, V. et al.
E2 and M1 Transition Probabilities in Odd Mass Hg Nuclei,
Nuclear Physics.

Berg, V., Malmskog, S.G. and Bäcklin, A.
The Level Structure in $^{193}$Ir,
Nuclear Physics.

Holmqvist, B. et al.
Neutron Scattering from Vanadium at 1.5 to 8 MeV,
Nuclear Physics.

Holmqvist, B. et al.
A Neutron Elastic Scattering Study of Chromium, Iron and Nickel in the Energy Region 1.77 to 2.76 MeV,
in manuscript.

Holmqvist, B. et al.
A Non-Spherical Optical Model Analysis of Fast Neutron Elastic Scattering from Tantalum,
Nuclear Physics.

Höglund, Å. and Malmskog, S.G.
Decay Characteristics of Levels in $^{151}$Eu,
Nuclear Physics.

Lodin, G.
Partial Differential Cross Sections of the $^{58}Ni(n, p)\ ^{58}Co$ Reaction at 3.06 and 3.65 MeV,
in manuscript.

Malmskog, S.G. and Berg, V.
Absolute Transition Rates in $^{188}Ir$,
Nuclear Physics.

Malmskog, S.G. and McDonald, J.
The 93.54 keV Level in $^{91}Sr$,
Nuclear Physics.

Malmskog, S.G. et al.
The Low Energy Level Structure of $^{191}Ir$,
Nuclear Physics.

Moxon, M, and Malmskog, S.G.
Precision (n, $\gamma$) Cross Sections of $^{238}U$ in the Energy Interval 5 eV to 200 keV,
in manuscript.

Moxon, M. and Malmskog, S.G.
The Resonance Integral for Si and SiC,
in manuscript.

Salama, M.
Fast Neutron Elastic Scattering Experiments,
in manuscript.

Tykesson, P. and Wiedling, T.
A Klystron Bunching System for a 6 MV Van de Graaff Accelerator,
Nuclear Instruments and Methods.